ENLOSS testing with HAM-Tools

SMHI Common exercise 0
Calculation of energy use for space heating

September 22, 2006

Angela Sasic Kalagasidis

Chalmers University of Technology
Department of Civil and Environmental Engineering
Building Physics Research Group
412 96 Gothenburg

Chalmers reference: Report number 2005:6, ISSN 1652-9162

Margitta Nord
Cari Andersson
Roger Teasler
Lena Gollvik

Swedish Meteorological and Hydrological Institute
Environment and Safety Service
601 76 NORRKÖPING

CONTENTS

1 INTRODUCTION

This report represents results of comparative testing of the building energy calculation program "Enloss", developed at the Swedish Meteorological and Hydrological Institute (SMHI) for studying the impact of weather and climate on building heating budget. The main task of the program is to calculate hourly heat losses and gains by taking into account combined action of outdoor temperature, wind and solar irradiation. Thermal inertia of a building, HVAC[1] systems and internal gains from occupants and electric appliances are also considered. With the forecast meteorological input to the calculations, the program gives predictions on the future heating energy demand (for five days), which are then used for the predictive control of a building heating system.

The testing of Enloss has been performed and conducted at the Building Physics Division, Chalmers University of Technology, Gothenburg, Sweden with the objective of suggesting possible improvements and further development of the program. To accomplish this, a detailed evaluation of the Enloss state-of-the-art calculations has been done by comparison with a benchmark program - HAM-Tools, developed at the Chalmers University of Technology, (Sasic, 2004).

HAM-Tools is a numerical program where the heating energy demand of a building is calculated directly from a system of energy balance equations for all components involved. The transient heat transfer through walls is calculated as one-dimensional process and the indoor air is treated as well mixed. The numerical solution is based on the control volume technique. Apart of being already validated (Sasic, in press), HAM-Tools is regarded as the appropriate benchmark program since it can use the input data in exactly the same way as Enloss does. Thus, equivalent calculation routines have been exercised using equivalent inputs and relevant outputs were directly compared: annual energy consumption of a building and hour-by-hour heating demand.

This report contains a detailed description of the test cases, selection of results produced by both of the programs and diagnostic technique which has been used to determine the algorithms responsible for the differences detected. The thermal model of a building, which is in-built in Enloss, is given in full by the set of mathematical equations. The testing has shown that the main difference between the programs is in the treatment of direct solar gains through windows. Therefore, alternative modelling approaches have been presented and discussed using HAM-Tools, which, in turn, showed possible improvements for Enloss towards more advanced modelling.

The results collected are provided on a compact disc. For information on the weather data please contact SMHI.

[1] An abbreviation for Heating, Ventilating and Air-Conditioning systems

2 TEST OBJECTIVES AND OVERVIEW

2.1 Test type: comparative

The common validation methodology of building energy simulation programs encloses three different kinds of tests, (Judkoff and Neymark, 1995):

- **Analytical verification**, where the output of a program is compared to the result of an exact analytical solution of the problem treated.

- **Comparative testing**, where the output of a program is compared to other programs or to itself.

- **Empirical validation**, where the output of a program is compared to measured data from a real structure or laboratory test facility.

Advantages and disadvantages of these testing techniques are summarized below.

Comparison with the analytical solution is the most correct test because a divergence from the solution, which is mathematically true, can be exactly evaluated. However, analytical solutions exist only for simple, rather theoretical cases and, accordingly, this test usually does not insure more than that a program produces correct numerical solution.

Comparative testing ensures that a program produces as accurate solutions as benchmark codes. This is a very powerful method of assessment since a lot of different test cases can be considered within a short time and inexpensively. The test is especially convincing when a program is validated against already well-established codes. The certainty of the test is relative - it is not a guarantee that the program is absolutely correct since it may be just as equally incorrect as benchmark programs.

Empirical validation shows up to what extent a code can predict the reality and, therefore, it is highly appreciated among program users. The certainty of the test significantly depends on the accuracy of the experiment. Measurements always involve uncertainties and their quality, when they represent input to simulations, determines the validation result. When doing such testing, it is very important that a program is suitable for the problems regarded in measurements, or the validation may fail. Measurements of high quality are expensive and time-consuming and therefore, the number of proper empirical tests is limited.

The testing of Enloss by HAM-Tools is the comparative testing.

The empirical validation of Enloss has also been performed by comparison between the measured and calculated heating energy use for a multi-storey residential building in Köping, Sweden. Results are enclosed in Appendix 7.

2.2 Test suite: SMHI common exercise 0

The “SMHI Common exercise 0” considers a basic thermal problem – the annual energy consumption of a model house. The test relies in great deal on the testing procedure known as “BESTEST” (Judkoff and Neymark, 1995), which is lately included in ANSI/ASHRAE Standard 140-2001. BESTEST provides methodology for a systematic testing of simulation

programs and for diagnosing of the sources of predictive disagreement. The method comprises a series of test case buildings that progress systematically from simple to relatively realistic ones. There are 36 cases in total, from which 14 are the qualification cases and the remaining ones are for diagnostic purposes.

"SMHI Common exercise 0" is based on two qualification cases from BESTEST, denoted as 600 and 900. The numbers refer to two buildings that are equal in size and have the same heat conductance, but differ in thermal mass - the lightweight building (600) and the heavyweight one (900). The buildings are simple in shape – a rectangular zone with no interior partitions, as shown in Figure 2, and thermally almost decoupled from the ground by thick floor insulation. Geometry and material specification are purposely simplified to minimize the opportunity for input errors (details can be found in Table 1-2).

2.2.1 Climate data

The cases 600 and 900 are intended for testing of a program's ability to model a thermal response of a house when subjected to solar heat gains through windows. In the original version, the test should be performed with the climate data from the Test Reference Year (TRY) of Denver, Colorado, USA, characterized by a hot summer and cold winter. In the SMHI Common exercise 0, the climate load is adjusted to the interest of the Enloss developers by using the Swedish climate data for Gothenburg[2]. The Gothenburg climate represents the southwest coastal area of Sweden (latitude 57.67 north, longitude 12.30 east, altitude 154 m) with mild summers and winters. The annual average air temperature for the site is 7.0 ^{o}C and the wind speed is 4.2 m/s. Other climate specifications may be found in Appendix 1. Ground temperature at the site is assumed constant and equal to 10°C.

2.2.2 Thermostat control strategies

Another deviation from the BESTEST testing conditions relates to the thermostat control strategies of the heating and cooling systems. Here, a constant indoor air temperature of 21^{o}C is assumed, corresponding to the so-called "bang-bang" control strategy:

heating = "on" if indoor air temperature is less than 21^{o}C
cooling = "on" if indoor air temperature exceeds 21^{o}C

The original cases 600 and 900 have a "dead-band" control system with two different temperatures:

heating = "on" if indoor air temperature is less than 20^{o}C
cooling = "on" if indoor air temperature exceeds 27^{o}C

At present, the Enloss model allows only the "bang-bang" control system. Both the heating and the cooling system are assumed with infinite heating (cooling) capacity, i.e. no time delay in heat delivery.

[2] SMHI measurements at Landvetter, 1991

2.2.3 Solar heat gains

Enloss considers only direct solar heat gains through windows. The significance of this free energy source on savings in heating energy demand is shown on two calculation exercises:

Case 1: house without solar gains through windows
Case 2: house with solar gains through windows

Case 1 may be interpreted as the heating energy demand of the house when its heating system is controlled by the outdoor air temperature, i.e. when free energy sources are neglected. Case 2 shows possible savings in heating energy demand by taking into account the solar gains.

2.2.4 Summary of test cases

By combining the climate data, type of the construction and the presence of the solar gains through windows, four test cases are obtained:

GBG-600-1 and GBG-900-1
Gothenburg climate, low and high mass buildings, without solar heat gains

GBG-600-2 and GBG-900-2
Gothenburg climate, low and high mass buildings, with solar heat gains through windows

2.2.5 The testing algorithm

The principle of comparative testing of ENLOSS with HAM-Tools is illustrated by the flow chart in Figure 1.

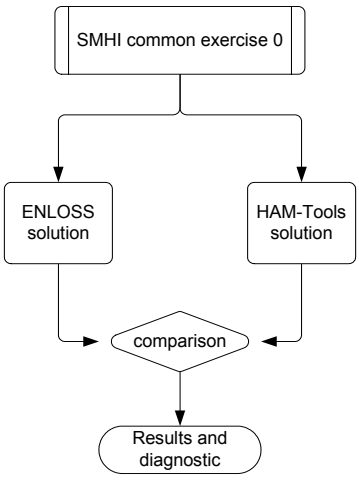

Figure 1 The flow chart of the validation method

3 INPUT DATA

3.1 Geometry and material specification for the test houses

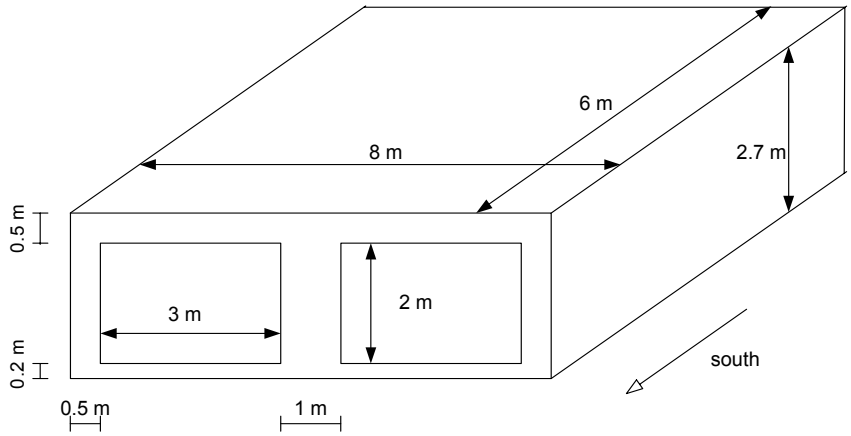

Figure 2 Geometry specification for the test building

Table 1 Thermal properties for the lightweight building (case 600)

Layer		K	d	U	R	ρ	c_p	Area
	Unit	W/mK	m	W/m^{2}K	m^{2}K/W	kg/m^3	J/kgK	m^2
Exterior wall	Plaster board	0.160	0.012	13.33	0.08	950	840	
	Fiberglass quilt	0.040	0.066	0.61	1.65	12	840	
	Wood siding	0.140	0.009	15.55	0.06	530	900	
	Total (U_o)			0.56	1.79			63.6
Floor	Timber flooring	0.140	0.025	5.60	0.18	650	1200	
	Insulation	0.040	1.003	0.04	25.07			
	Total (U_o)			0.04	25.25			48.0
Roof	Plaster board	0.160	0.010	16.00	0.06	950	840	
	Fiberglqss quilt	0.040	0.112	0.36	2.79	12	840	
	Wood siding	0.140	0.019	7.37	0.14	530	900	
	Total (U_o)			0.33	3.00			48.0

Table 2 Thermal properties for the heavyweight building (case 900)

Layer		K	d	U	R	ρ	c_p	Area
	Unit	W/mK	m	W/m^{2}K	m^{2}K/W	kg/m^3	J/kgK	m^2
Exterior wall	Concrete block	0.510	0.100	5.10	0.20	1400	1000	
	Foam insulation	0.040	0.062	0.65	1.54	10	1400	
	Wood siding	0.140	0.009	15.56	0.06	530	900	
	Total (U_o)			0.56	1.80			63.6
Floor	Concrete slab	1.130	0.080	14.12	0.07	1400	1000	
	Insulation	0.040	1.007	0.04	25.17			
	Total (U_o)			0.04	25.25			48.0
Roof	Plaster board	0.160	0.010	16.00	0.06	950	840	
	Fiberglqss quilt	0.040	0.112	0.36	2.79	12	840	
	Wood siding	0.140	0.019	7.37	0.14	530	900	
	Total (U_o)			0.33	3.00			48.0

Overall heat conductance for windows is U_o = 3.0 W/m^{2}K.

3.2 Thermal time constant of the test houses

In ENLOSS, the dynamical heat storage in construction elements of the test house is accounted for by its thermal time constant. There are two different values for this parameter (τ, Table 3), one for the lightweight house (600) and the other for the heavy weight one (900). The time constants used in this testing are defined and evaluated according to the standard EN ISO 13790:2004. The calculation procedure for τ and the way it is used in ENLOSS is given in Appendix 2.

Table 3 Time constants for the test houses

Construction type	600	900
τ (h)	5	26

3.3 Specific input information

3.3.1 Exterior surface transfer coefficient

Heat transfer coefficient on the exterior side is given by:

$$\alpha_{out} = 6.4 \cdot \frac{w_r^{0.6}}{D^{0.4}} + \frac{20.8}{10^8} \cdot T_{out}^3 \qquad \text{W/m}^2\text{K} \qquad (1)$$

where D (m) is the mean of the house width and length (D=7 m), T_{out} (K) is the outdoor air temperature and w_r (m/s) is the wind speed at the height of the house r = 2.7 m.

The wind speed is calculated according to the ENLOSS model, described in Appendix 3. For the open flat position of the house, the following relation is valid:

$$w_r = 0.709 \cdot w_{10} \qquad \text{m/s} \qquad (2)$$

where w_{10} is the wind speed measured at 10 m.

The first term on the right-hand side in Equation 1 represents the convective heat transfer coefficient, while the second one accounts for the long-wave radiative heat exchange (Taesler, 1986). For the annual mean outdoor air temperature of 7°C and the mean wind speed of 4.2 m/s at 10 m, the mean value of the outdoor heat transfer coefficient is α_{out}=10.2 W/m^{2}K.

3.3.2 Interior surface transfer coefficient

$$\alpha_{in} = \frac{20.8}{10^8} \cdot T_{in}^3 \qquad \text{W/m}^2\text{K} \qquad (3)$$

where T_{in} (K) is the indoor air temperature. For a constant indoor air temperature of 21°C, α_{in}=5.2 W/m^{2}K.

3.3.3 Windows

Solar heat gains through windows are based on the fenestration area, i.e. the window glass area plus the framing. The glass transmittance is given constant τ_w = 0.6 (-) and the shading factor (known in ENLOSS as the function of Venetian blinds, Appendix 6) is s = 1 (-).

3.3.4 Ventilation

The house is mechanically ventilated with outdoor air and the constant ventilation airflow rate of 0.5 h^{-1} is applied. The house is assumed airtight.

3.3.5 Internal heat gains

Internal heat gains constantly generate 200 W.

4 REQUIRED OUTPUTS

4.1 Definition of areas and volumes

Windows area	$A_{window} = 12\ m^2$
Wall area without windows	$A_{wall} = 63.6\ m^2$
Roof and floor area	$A_{roof} = A_{floor} = 48\ m^2$
Total area	$A_{total} = A_{window} + A_{wall} + A_{roof} + A_{floor} = 171.6\ m^2$
Total volume	$V_{total} = 129.6\ m^3$

In ENLOSS, all heat loses are expressed using the heated floor area, which is defined as 87 % of the total floor area:

BOA area	$A_{BOA} = 0.87 \cdot A_{floor} = 42\ m^2$
BOA volume	$V_{BOA} = V_{total} \cdot 0.87\ m^3 = 112.7\ m^3$

4.2 Hourly outputs

4.2.1 Heat losses through walls

$$q_{trans}(t) = \frac{1}{A_{BOA}} \cdot \sum_{i} U_i \cdot (T_{in} - T_{out}(t)) \cdot A_i \qquad W/m^2_{BOA} \qquad (4)$$

where index *i* refers to walls, roof and windows and *t* is time. U_i (W/m^{2}K) is the total ("air to air") heat conductance for the construction element concerned:

$$\frac{1}{U_i} = \frac{1}{\alpha_{out}} + \frac{1}{U_{o,i}} + \frac{1}{\alpha_{in}} \qquad m^2K/W \qquad (5)$$

where $U_{o,i}$ (W/m^{2}K) is the nominal ("surface-to-surface") heat conductance from Table 1-2.

4.2.2 Heat losses through the ground

$$q_{ground}(t) = \frac{1}{A_{BOA}} \cdot U_{o,floor} \cdot (T_{in} - T_{ground}) \cdot A_{floor} \qquad W/\ m_{BOA}^2 \qquad (6)$$

where $T_{ground} = 10^oC$.

4.2.3 Heat losses due to ventilation

$$q_{vent}(t) = \frac{1}{A_{BOA}} \cdot \frac{n \cdot \rho_{air} \cdot c_{p,air}}{3600} \cdot (T_{in} - T_{out}(t)) \cdot V_{BOA} \quad \text{W/m}_{BOA}^2 \quad (7)$$

where n (ach) is the number of air changes per hour, ρ_{air} (1.2 kg/m^3) and $c_{p,air}$ (1000 J/kgK) are the air density and the specific heat capacity.

4.2.4 Solar gains through windows

$$q_{sol.window}(t) = \frac{1}{A_{BOA}} \cdot \tau_w \cdot s \cdot (I_{dir}(t) + I_{diff}(t)) \cdot A_{window} \quad \text{W/mBOA2} \quad (8)$$

where I_{dir} and I_{diff} are direct and diffuse solar irradiation on the glazing.

4.2.5 Internal gains

$$q_{in} = 200 \ \text{W/m}_{BOA}^2 \quad (9)$$

4.2.6 Heating and cooling energy demand

Heating energy demand for the house is defined as the heat needed to maintain the given indoor air temperature. By summing all heat gains and losses for each hour (as they are defined in Sections 4.2.1-5):

$$q_n(t) = q_{trans}(t) + q_{ground}(t) + q_{vent}(t) - q_{sol,window}(t) - q_{in} \quad \text{W/m}_{BOA}^2 \quad (10)$$

the heating demand is defined as the positive value of the sum, i.e. whenever the heat gains do not compensate the heat losses. The negative value of the sum defines the cooling demand:

$$q_{heating}(t) = q_n(t) \ \text{ if } q_n(t) > 0 \quad \text{W/m}_{BOA}^2 \quad (11)$$

$$q_{cooling}(t) = q_n(t) \ \text{ if } q_n(t) < 0$$

4.3 Annual outputs

Results are reported also in the form of the annual heating and cooling energy demand:

$$Q_{heating} = 0.001 \cdot \sum_{j=0}^{8760} q_{heating}(t_j) \quad \text{kWh/m}_{BOA}^2 \qquad (12)$$

$$Q_{cooling} = 0.001 \cdot \sum_{j=0}^{8760} q_{cooling}(t_j) \quad \text{kWh/m}_{BOA}^2 \qquad (13)$$

where j is the hour in a year and 8760 is the total number of hours in one year.

4.4 Enloss features not included in this testing

The model for air-infiltration through cracks and leakages on building facades and the one for sun shading devices on windows (so called the function of Venetian blinds) are not used in this testing. However, these features are commonly used in practice, as it is shown in the empirical validation test (Appendix 7). For that reason, full models of these are given in Appendices 5 and 6.

5 RESULTS OF THE TESTING

5.1 Case 1: No solar gains

Results obtained by both programs are in excellent agreement. The annual demands are summarized in Table 4 and hourly values are given in Figure 4 for the two characteristic periods: during the coldest days in the year, February 14-16, and during half-cloudy days in autumn (September 24-26) with high wind speed and moderate outdoor temperature.

5.2 Case 2: Solar gains through windows

Results obtained by both programs are generally in good agreement, but with some differences in exact numbers: the calculated cooling energy demands are very close, but Enloss shows lower heating energy demand in comparison to the results of HAM-Tools. The results are summarized in Table 5 and 6 and in Figures 5 and 6. The cause of the difference is explained hereafter.

5.2.1 Reasons for the differences

As discussed in the paper that followed this testing (Appendix 8), the cause of the differences between Enloss and HAM-Tools solutions for Case 2 is in the treatment of the solar gains through windows. In Enloss, the solar gains are not separated from other heat gains and losses in the heat budget equation 10 (Section 4.2.6)

$$q_n(t) = q_{trans}(t) + q_{ground}(t) + q_{vent}(t) - q_{sol,window}(t) - q_{in} \qquad \mathrm{W/m}_{BOA}{}^2$$

where the different terms are defined according to Sections 4.2.1-5, Equations 4 and 6-9.

In order to account for the dynamic heat storage in walls, the weighted (smoothed) net heat input is produced as the moving weighted average of the hourly $q_n(t)$:

$$q_{smooth}(t) = q_n(t) + \sum_{m=1}^{\tau} \Delta q_n(m) \cdot e^{-m/\tau} \left(1 - e^{-m/\tau}\right) \qquad (14)$$

where t is the present (selected) time step, m (h) is the number of backward steps, $\Delta q_n(m) = q_n(t-m) - q_n(t)$ is the difference in the heat input between the previous and the present time step and τ is the thermal time constant of the house. Since the solar gains are included in the net heat input $q_n(t)$ (Equation 10), they are weighted with the time constant of the house.

In the HAM-Tools model for Case 2, the solar gains are treated as the radiative heat sources, i.e. as the energy source that first reaches and warms up the interior surfaces and thereby, the air, as it is illustrated in Figure 3. It is assumed here that the solar radiation is uniformly distributed between the surfaces (the same is valid for Enloss), but the difference in thermal capacity of the construction elements is taken into account.

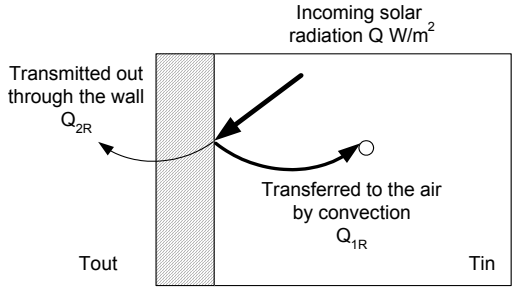

Figure 3: The radiative model for direct solar gains, as it is used in the HAM-Tools calculations.

It is possible to achieve excellent agreement between the solutions by using the more accurate weighting method for the solar gains. The energy balance equation 10 is firstly rewritten into:

$$q_n(t) = q_n^*(t) - q_{sol,window}(t) \tag{15}$$

where $q_n^*(t)$ contains all losses and gains except the solar gains:

$$q_n^*(t) = q_{trans}(t) + q_{ground}(t) + q_{vent}(t) - q_{in}(t) \tag{16}$$

Secondly, $q_{smooth,1}(t)$ is calculated as the weighted $q_n^*(t)$ and $q_{sol,smooth}(t)$ as the weighted $q_{sol,window}(t)$:

$$q_{smooth,1}(t) = q_n^*(t) + \sum_{m=1}^{\tau} \Delta q_n^*(m) \cdot e^{-m/\tau}\left(1 - e^{-m/\tau}\right) \tag{17}$$

$$q_{sol,smooth}(t) = \sum_i \sum_{m=1}^{M_i} \kappa_{sol,i}(t-m) \cdot q_{sol,window}(m) \tag{18}$$

While $q_n^*(t)$ is weighted with the same weighting factors as $q_n(t)$ in Equation 14, $q_{sol,window}(t)$ is weighted with separately calculated solar-weighting factors $\kappa_{sol,i}$. The solar-weighting factors $\kappa_{sol,i}$ and the total number of backward steps M_i (-) are different for each of the construction elements i; since all elements contribute to the heat transfer, the summation is performed for all of them. The whole procedure is shown through examples included in Appendix 4, as well as the results obtained.

Finally, the total smoothed net heat input is represented as:

(19)

The difference between $q_{smooth}(t)$ and $q^{*}_{smooth}(t)$ is the difference that is seen in Figure 5 and 6. Therefore, the difference between the solutions for Case 2 is due to the lumped character of the Enloss model, where thermally different construction elements are represented by a single parameter – the thermal time constant of the house. Unlike from the outdoor air temperature, variations in solar radiation intensity during the day are of several orders of magnitudes. This implies that the accuracy of weighting procedure is more important for the calculation of direct solar gains than for the calculation of transmittion heat losses. In Case 1, where the solar gains are zero, Equations 17 and 19 lead to the same results.

The modelling procedure for direct solar gains can be further developed by taking into account the long-wave radiation exchange between internal surfaces, the more exact distribution of solar gains between surfaces, etc. At the present stage of the model development this is not considered necessary since the most of input data required thereby are usually not available.

Table 4 Results for Case 1: No solar radiation on surfaces or through windows

Unit: kWh/m_{BOA}^2	GBG-600-1		GBG-900-1	
	Enloss	HAM-Tools	Enloss	HAM-Tools
Losses: windows + walls + roof	188.0	188.3	187.6	187.7
Floor	4.5	4.3	4.5	4.3
Ventilation	55.4	55.1	55.4	55.1
Sum losses	247.8	247.7	247.4	247.1
Direct solar gains	0	0	0	0
Internal gains	42.0	41.7	42.0	41.7
Heating demand	206.9	207.4	205.8	206.1
Cooling demand	1.1	2.6	0.4	1.8

Table 5: Results for Case 2: Solar radiation through windows

Unit: kWh/m_{BOA}^2	GBG-600-2		GBG-900-2	
	Enloss	HAM-Tools	Enloss	HAM-Tools
Losses: windows + walls + roof	188	104.5	187.6	96.3
Floor	4.5	1.2	4.5	0.2
Ventilation	55.4	55.1	55.4	55.1
Sum losses	247.8		247.4	
Direct solar gains	155.1	155.7	155.1	155.7
Internal gains	42.0	41.7	42.0	41.7
Heating demand	146.7	155.5	113.9	127.6
Cooling demand	96.1	95.0	63.6	67.5

Table 6: Relative differences in annual energy demands. HAM-Tools vs.Enloss.

	GBG-600	GBG-900
Heating demand	-5.6 %	-10.7 %
Cooling demand	+1.1 %	-5.8 %

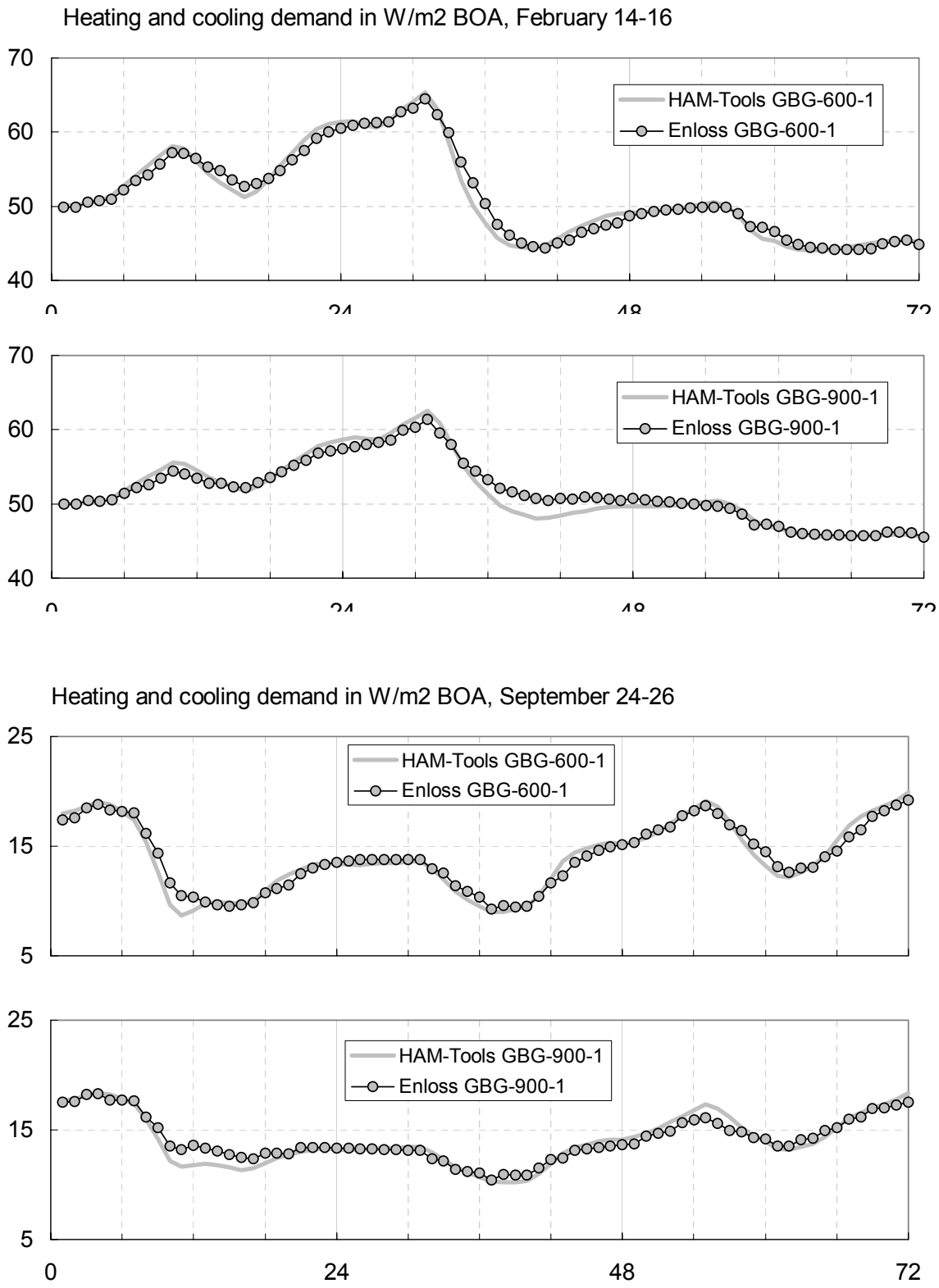

Figure 4: Hourly heating / cooling energy demands for the test cases GBG-600-1 and GBG-900-1.

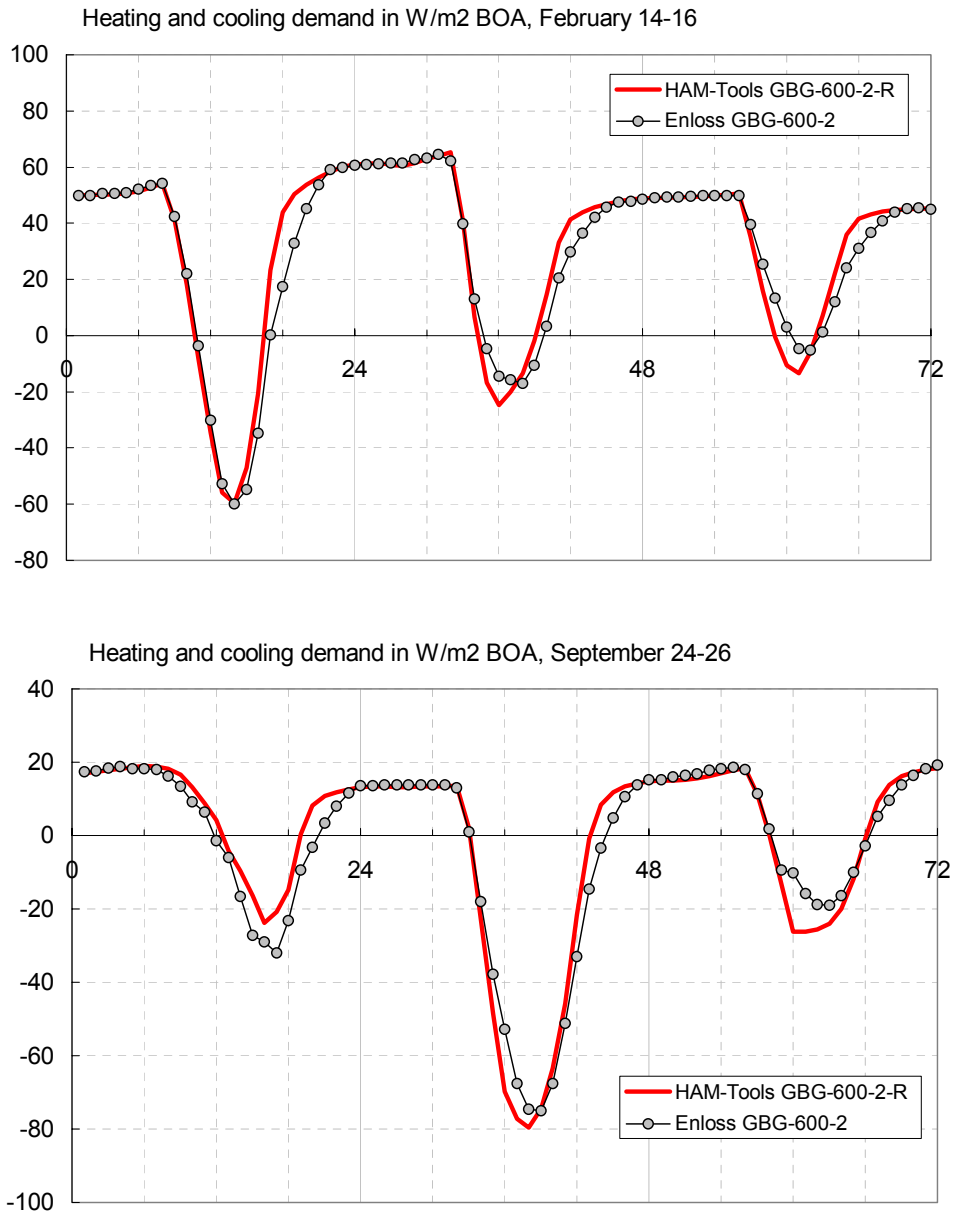

Figure 5: Hourly heating / cooling energy demands for the test cases GBG-600-2.

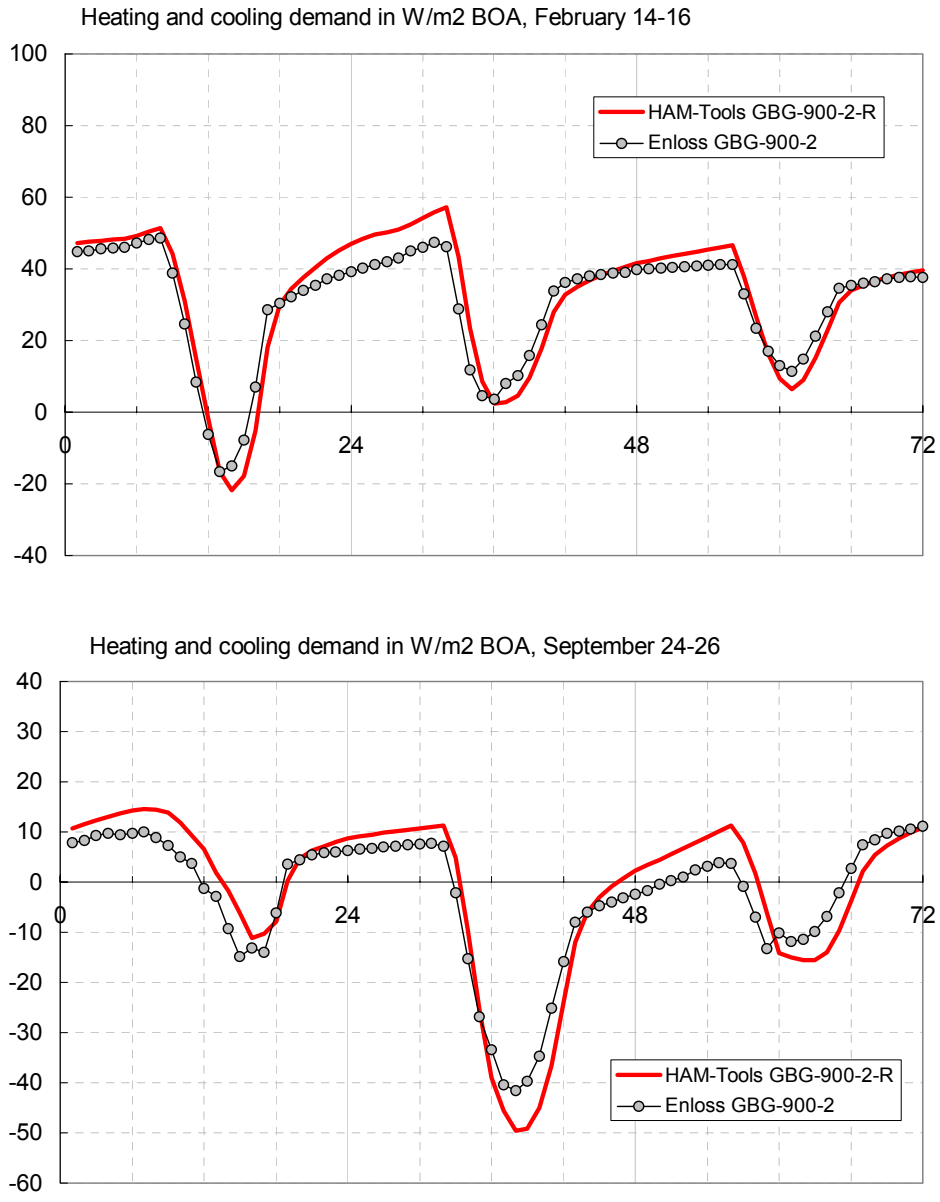

Figure 6: Hourly heating / cooling energy demands for the test cases GBG-900-2.

6 SURFACE HEAT TRANSFER COEFFICIENTS USED

The Enloss models for the external and internal transfer coefficients yield to lower values (see sections 3.3.1 and 3.3.2) than the ones used in the standard calculations (EN ISO 13790):

Enloss external: 10.2 W/m^{2}K on average (7^{o}C, 4.2 m/s)
Standard external: 25 W/m^{2}K

Enloss internal: 5.2 W/m^{2}K for the indoor air temperature of 21^{o}C
Standard internal: 7.69 W/m^{2}K.

This means that Enloss calculates the lower heat transfer rate between the outdoor / indoor air and outdoor / indoor surfaces than what standard calculations do, dampening the effects of both heat gains and heat losses. This chapter gives a short overview of the models commonly used for the heat transfer coefficients and some results obtained by these for Case 2-R.

6.1 Internal surface transfer coefficient

The internal surface film coefficient controls transfers of heat generated within a building to the building surfaces. It consists of a combination of convective and radiative components:

$$\alpha_{in} = \alpha_{in,c} + \alpha_{in,r} \tag{20}$$

The convective heat transfer coefficient $\alpha_{in,c}$ depends on the direction of the heat flow, the air flow at the surface and on the temperature difference between the air and the wall surface. The radiative transfer coefficient $\alpha_{in,r}$ depends on the radiative interactions between the surface under investigation and all other surfaces in the room. The most realistic values of the total thermal transfer coefficients, based on the mean radiant temperature in the room, are shown in Table 7 (Sanders, 1996). The values are based on theoretical and empirical studies and more details can be found in (IEA 14).

In BESTEST, the combined surface coefficient is given according surface orientation and infrared emissivity, Table 8, where the radiative part of these coefficients may be taken as 5.13 W/m^{2}K for the surfaces with an infrared emissivity of 0.9 and 0.57 W/m^{2}K for the emissivity of 0.1. If the program does not allow the setting up of these coefficients, it is recommended to use 8.29 W/m^{2}K (3.73 W/m^{2}K if emissivity is 0.1) also for horizontal surfaces.

6.2 External surface transfer coefficient

The outside surface thermal film coefficient can be also presented as the combination of the convective and the radiative coefficients. In Sanders (1996), the values shown in Table 9 are proposed for three exposure ratings:

- Sheltered – up to the third floor in the city centre
- Normal – mostly suburban and rural buildings; fourth to eighth floors of city centre buildings
- Exposed – coastal or hill top sites, floors above fifth in suburban sites or above eighth in city centres.

Table 10 summarizes the values for this coefficient according to BESTEST.

6.3 Energy consumption with the BESTEST surface transfer coefficients

Case 2-R is recalculated by HAM-Tools using the constant (BESTEST) heat transfer coefficients from Table 8. The results are shown in Table 11 and Figures 10-12, together with the ones obtained with the Enloss heat transfer coefficients from section 5.2.2. The higher heat transfer rate affects more the heavyweight building leading to higher energy demand. Taking into account the uncertainties involved in modelling of the heat transfer coefficients, the differences between the models are not distinct enough to question the Enloss model.

Table 7: Internal heat transfer coefficients

Location	α_{in} W/m^{2}K
In the centre of unobstructed surfaces – walls	8
ceiling	10
floor	7
In a two dimensional corner	6
In a tree dimensional corner	4
Behind furniture with no air flow	2

Table 8: Internal heat transfer coefficients according BESTEST

Orientation of surface and heat flow	α_{in} W/m^{2}K	
	Surface emissivity 0.9	Surface emissivity 0.1
Horizontal heat transfer on vertical surfaces	8.29	3.73
Upward heat transfer on horizontal surfaces	9.26	4.70
Downward heat transfer on horizontal surfaces	6.13	1.57
Upward heat transfer on 45^o surfaces	9.09	4.53
Downward heat transfer on 45^o surfaces	7.50	2.94

Table 9: External surface transfer coefficients according Sanders, 1996

Building element	Surface emissivity	Combined surface coefficient α_{out} W/m^{2}K		
		Sheltered	Normal	Exposed
Wall	High	12	16	33
	Low	9	14	33
Roof	High	14	25	50
	Low	11	20	50

Table 10: External surface transfer coefficients according BESTEST

Surface texture	Combined surface coefficient α_{out} W/m^{2}K	
	Surface emissivity 0.9	Surface emissivity 0.1
Brick or rough plaster	29.3 (all walls and roofs)	25.2 (all walls and roofs)
Glass or very smooth surface	21.0 (window and high-conductive wall)	16.9 (window and high-conductive wall)

Table 11: HAM-Tools results for Case 2-R with the BESTEST surface transfer coefficients

Unit: kWh/m$_{BOA}^2$	GBG-600	GBG-900		
Losses: windows + walls + roof				
Floor				
Ventilation	55.1	55.1		
Sum losses				
Direct solar gains	155.7	155.7	Comparison with results from Table 6	
Internal gains	41.7	41.7	GBG-600	GBG-900
Heating demand	162.2	137.8	+ 4.3 %	+ 8.0 %
Cooling demand	96.7	72.7	+ 1.2 %	+ 7.7 %

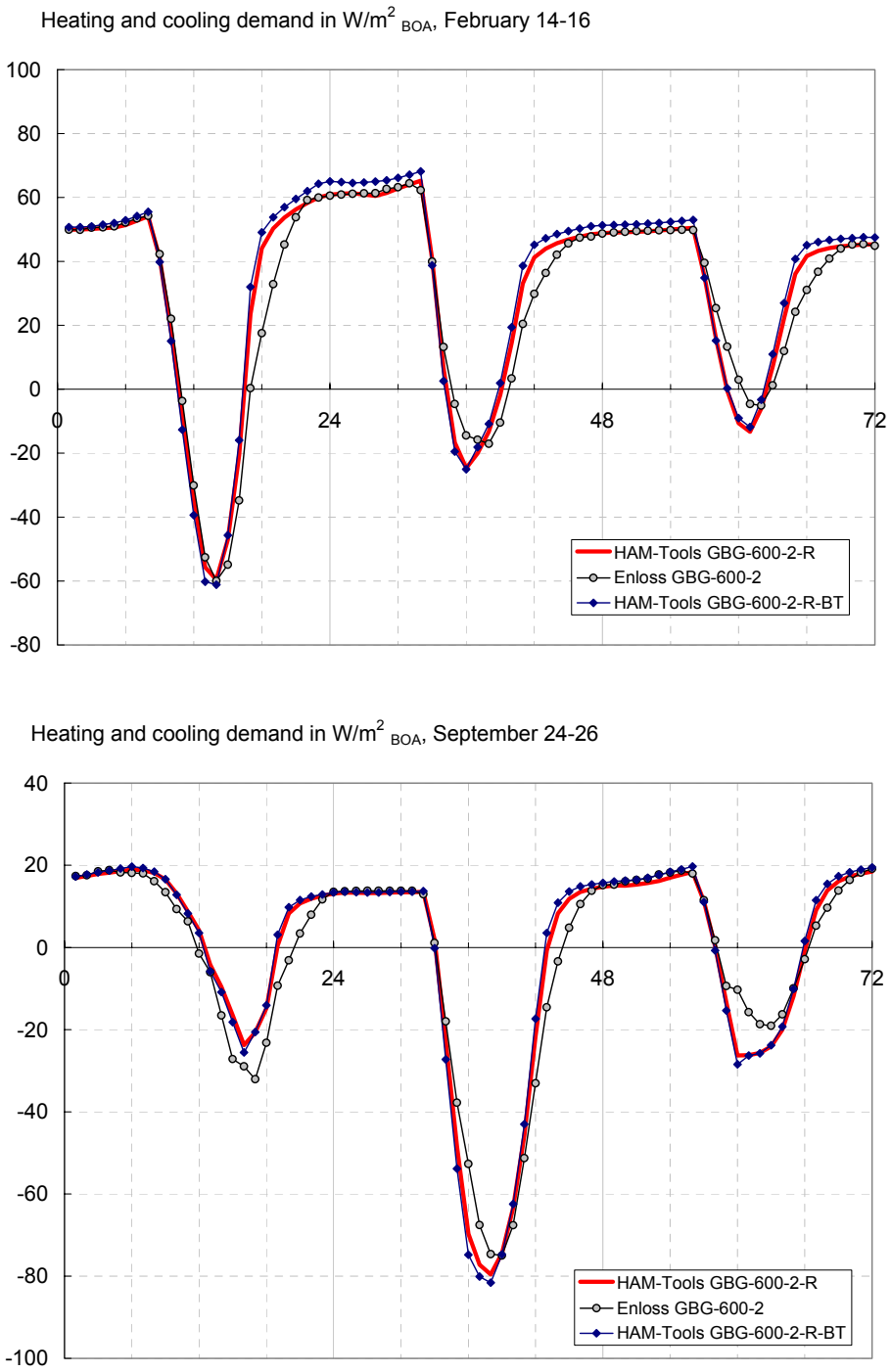

Figure 7 Hourly heating / cooling energy demands for Case GBG-600-2-R. Comparison between the Enloss and the BESTEST model (2-R-BT) for the heat transfer coefficients. Enloss results for Case GBG-600-2 are given as the reference.

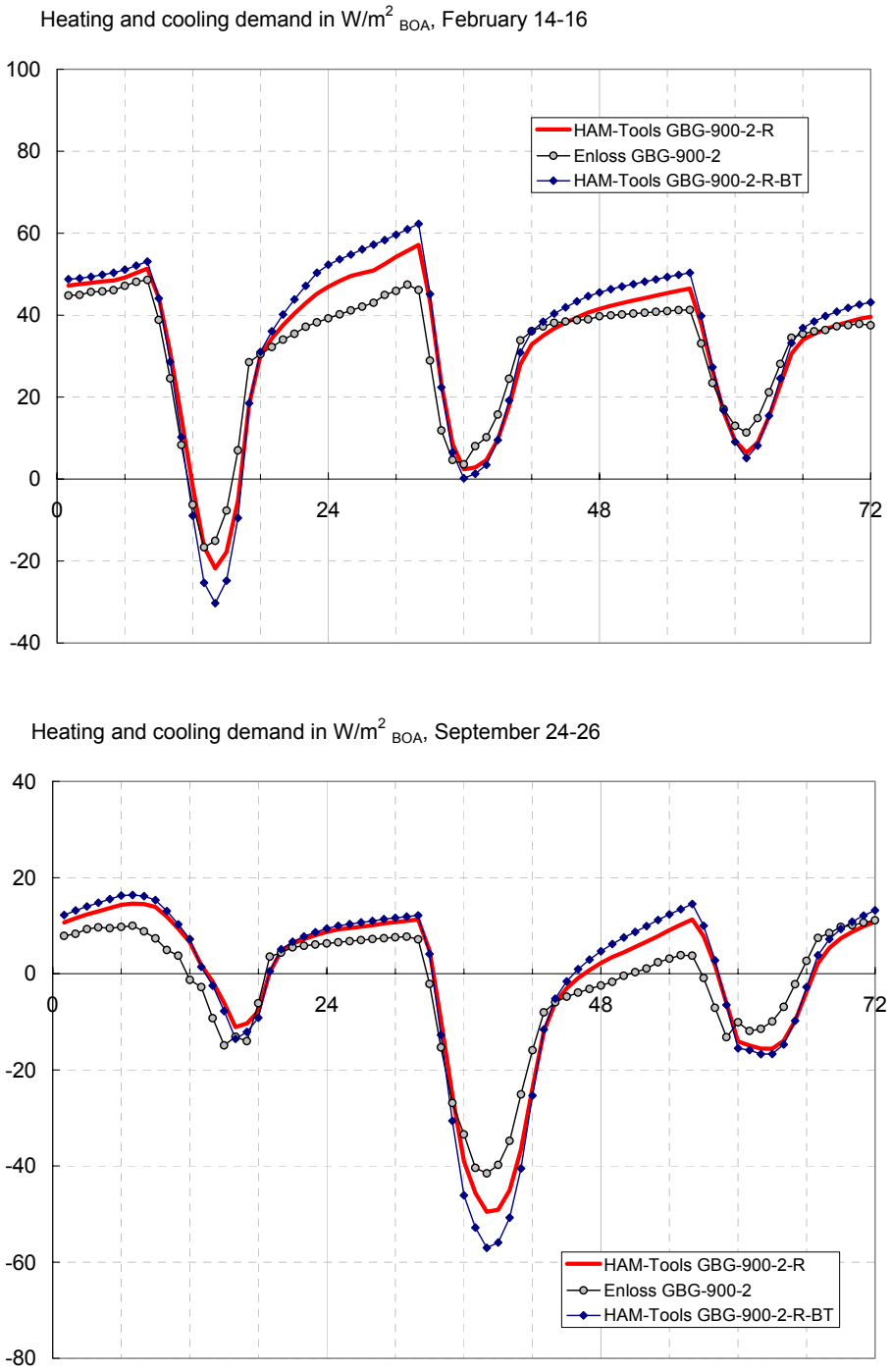

Figure 8 Hourly heating / cooling energy demands for Case GBG-900-2-R. Comparison between the Enloss and the BESTEST model (2-R-BT) for the heat transfer coefficients. Enloss results for Case GBG-600-2 are given as the reference.

7 FEATURES OF INTEREST FOR ENERGY CALCULATIONS AND NOT INCLUDED IN ENLOSS

7.1 Solar irradiation on facades

In the present version of Enloss, the effects of solar irradiation on facades are neglected. There are lot of uncertainties on how much of this irradiation reaches the building due to, sometimes, very complicated geometry and surroundings. Therefore, the effect of this free energy source on heating and cooling demand of a building may range from significant to negligible. The similar type of uncertainty can also be addressed to direct solar gains through windows.

In case of the test houses, these so-called indirect solar gains have significant influence on the energy demand due to the well-exposed location of the houses. This is illustrated by the following calculation example - Case 3 (i.e. GBG-600-3 and GBG-900-3). The radiative model for solar gains through windows is used in these calculations (see section 5.2.2). Effects of variable outdoor air temperature and wind speed are excluded by using the constant heat transfer coefficients from BESTEST. The solar irradiation on facades is calculated by taking into account the orientation and tilt of walls and roof.

Results for Case 3 (Table 12) indicate small effects (savings) in the heating energy demand, but also show more than a doubled cooling demand. Hourly-values are shown in Figure 9 and 12. The following model explains the difference between Case 2-R and Case 3, in a simplified way.

The indirect solar gains can be implemented via the so-called solar-air temperature; its value (T_{sol}) is obtained as the equivalent outdoor temperature from the following energy balance equation:

$$\alpha_{out} \cdot \left[T_{sol}(t) - T_{surf}(t)\right] = \alpha_{out} \cdot \left[T_{out}(t) - T_{surf}(t)\right] + a_b \left[I_{dir}(t) + I_{diff}(t)\right] \qquad (21)$$

where T_{surf} is the temperature of the surface, α_{out} is the combined external surface coefficient, a_b is the surface absorptivity (0.6 for opaque surfaces and 0 for windows) and I_{dir} and I_{diff} net direct and diffuse solar irradiance on the surface. After some algebra, the equation for the solar-air temperature reads:

$$T_{sol}(t) = T_{out}(t) + \frac{a_b}{\alpha_{out}} \left[I_{dir}(t) + I_{diff}(t)\right] \qquad (22)$$

With $a_b / \alpha_{out} = 0.02$, each 100 W/m^2 will increase the outdoor air temperature for 2 ^{o}C.

Table 12 HAM-Tools results for Case 3

Unit: kWh/m_{BOA}^2	GBG-600	GBG-900		
Losses: windows + walls + roof				
Floor				
Ventilation	55.1	55.1		
Sum losses				
Direct solar gains	155.7	155.7	Comparison with results from Table 12	
Internal gains	41.7	41.7	GBG-600	GBG-900
Heating demand	149.4	119.1	- 8 %	-13.6 %
Cooling demand	206.2	176.3	+ 113.2 %	+ 142.5 %

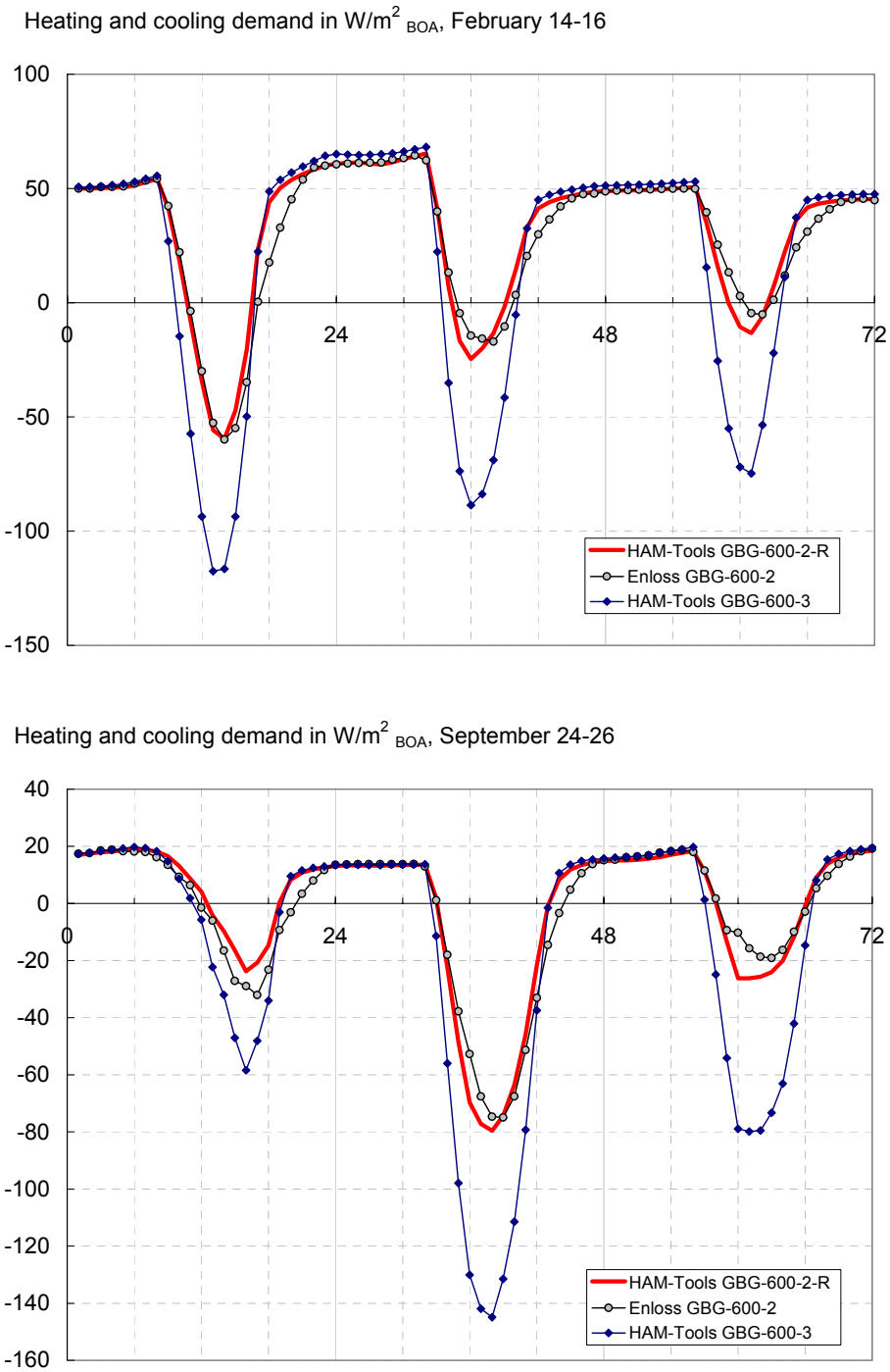

Figure 9 Hourly heating / cooling energy demands for Case 3 (GBG-600). Enloss results for Case 2 and HAM-Tools results for Case 2-R are given as the references.

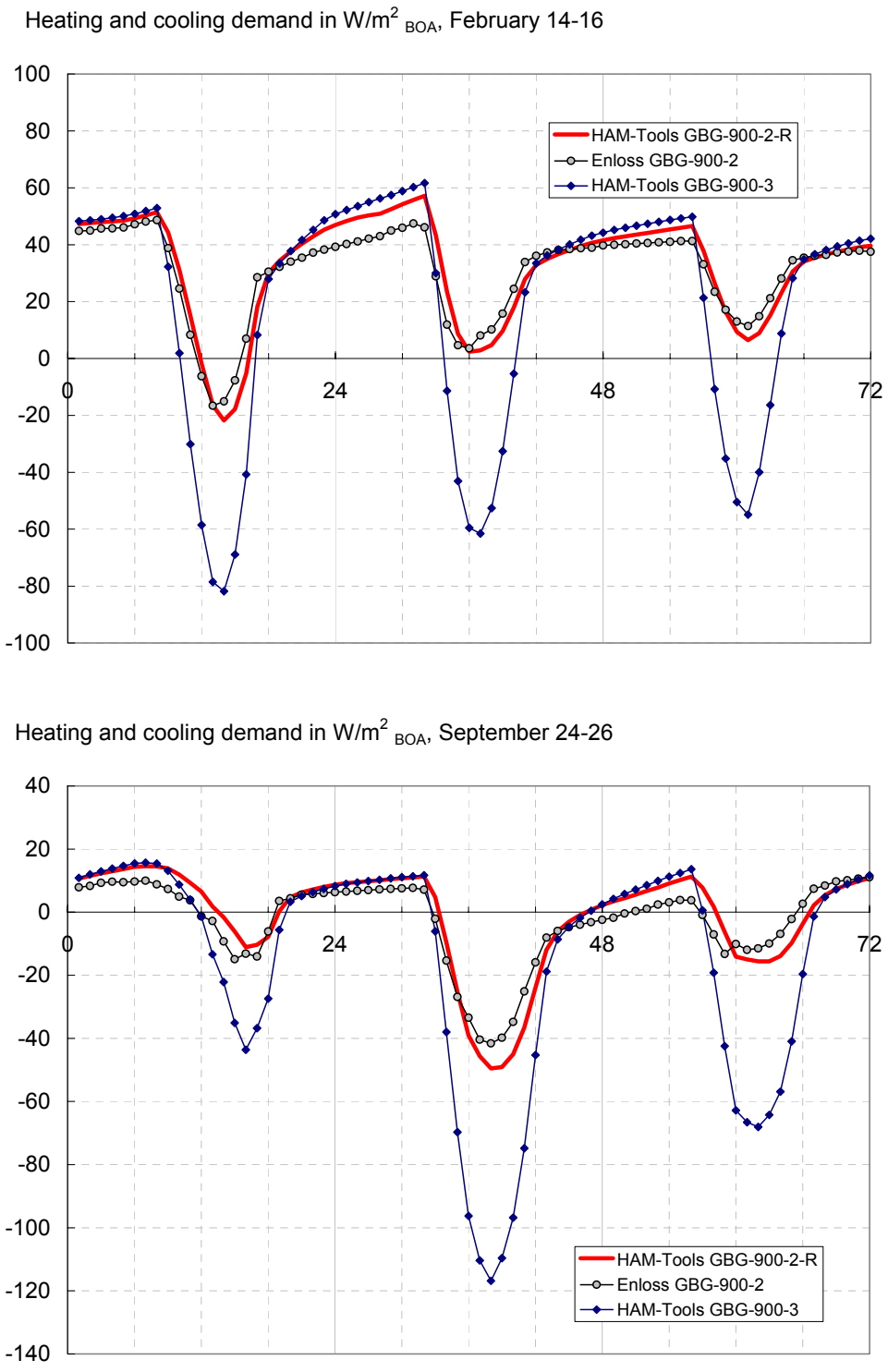

Figure 10 Hourly heating / cooling energy demands for Case 3 (GBG-900). Enloss results for Case 2 and HAM-Tools results for Case 2-R are given as the references.

7.2 Two-level thermostat control strategies

A good thermal comfort is normally fulfilled within a range of indoor air temperatures. It is required that the temperature does not go below a certain value, for example 21°C, but it can be higher than that – up to 26-28 °C, when the need for cooling is expected appear. From the energy demand point of view, this means that a lot of energy for cooling can be saved by avoiding cooling within the range of thermal comfort. This is will be illustrated with the next calculation exercise, which is the same as Case 3 except that the cooling set-point temperature is 26°C.

Annual energy inputs are summarized in Table 13 and compared to the previous case with the set point temperature for cooling 21°C. There are substantial savings in both cooling and heating energy demand for the heavyweight house, because the variable indoor air temperature allows the storing of heat in the construction. The energy savings for the lightweight house are only in the cooling area.

Apart from positive effects of the two-levelled temperature control systems, there are also some problems for the control system which can come into unstable operating regime. Instead of having a rather smooth change in the energy demand, the broken line that appears in Figure 11 and 14 indicates that the control system has undergone a lot of on / off switchings in a short time and in certain periods of the day. However, this is a common feature and usually well treated in automatic controlling.

Table 13 HAM-Tools results for Case 3 and the set point temperatures 21/26 °C

Unit: kWh/m_{BOA}^2	GBG-600	GBG-900		
Losses: windows + walls + roof				
Floor				
Ventilation	55.1	55.1		
Sum losses				
Direct solar gains	155.7	155.7	Comparison with results from Table 13	
Internal gains	41.7	41.7	GBG-600	GBG-900
Heating demand	143.3	88.6	- 4 %	- 25.6 %
Cooling demand	166.4	106.9	- 19.3 %	- 39.4 %

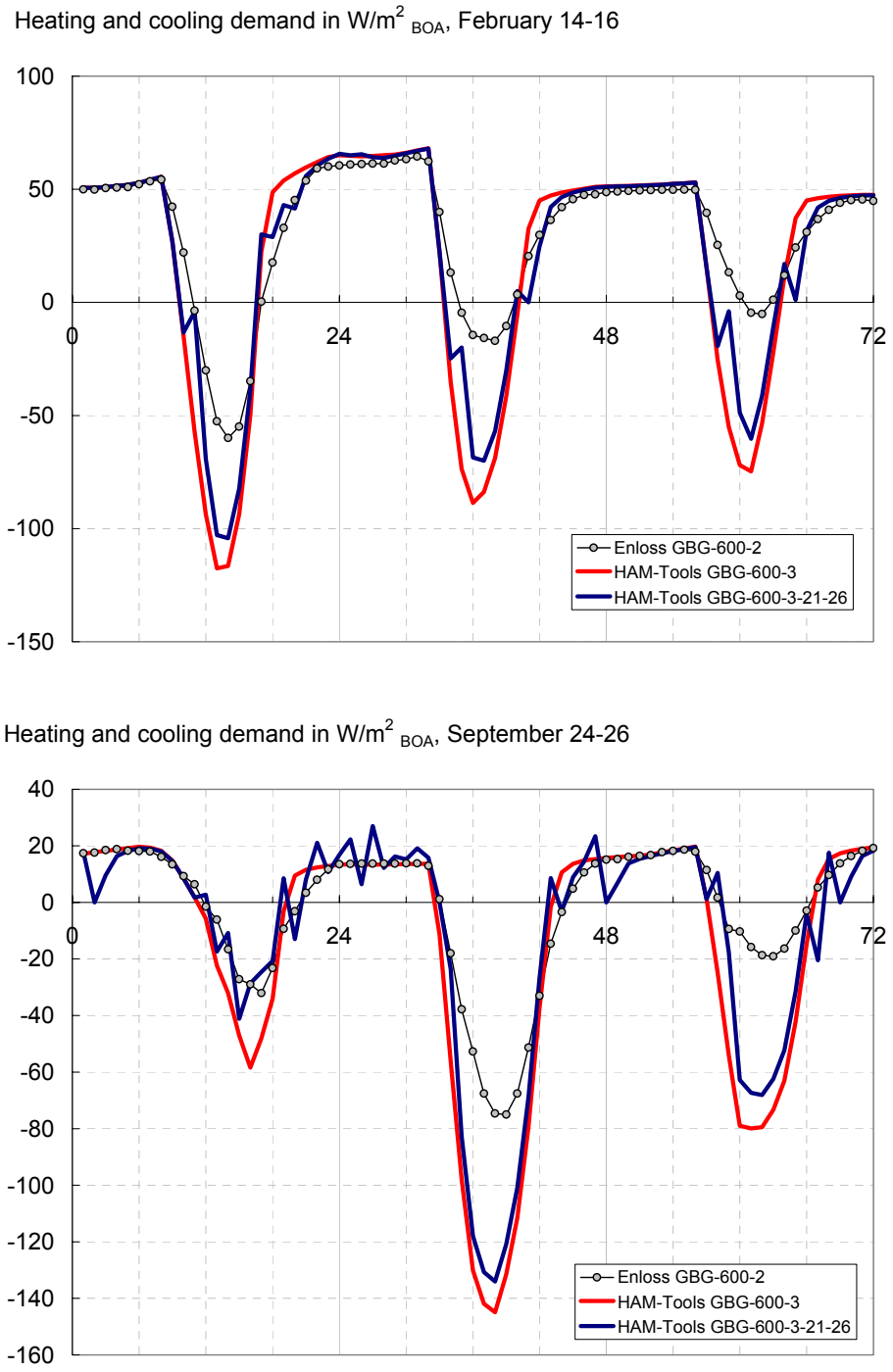

Figure 11 Hourly heating / cooling energy demands for Case 3 with two different heating / cooling set point temperatures: 21/21 °C and 21/26 °C (GBG-600). Enloss results for Case 2 are given as the reference.

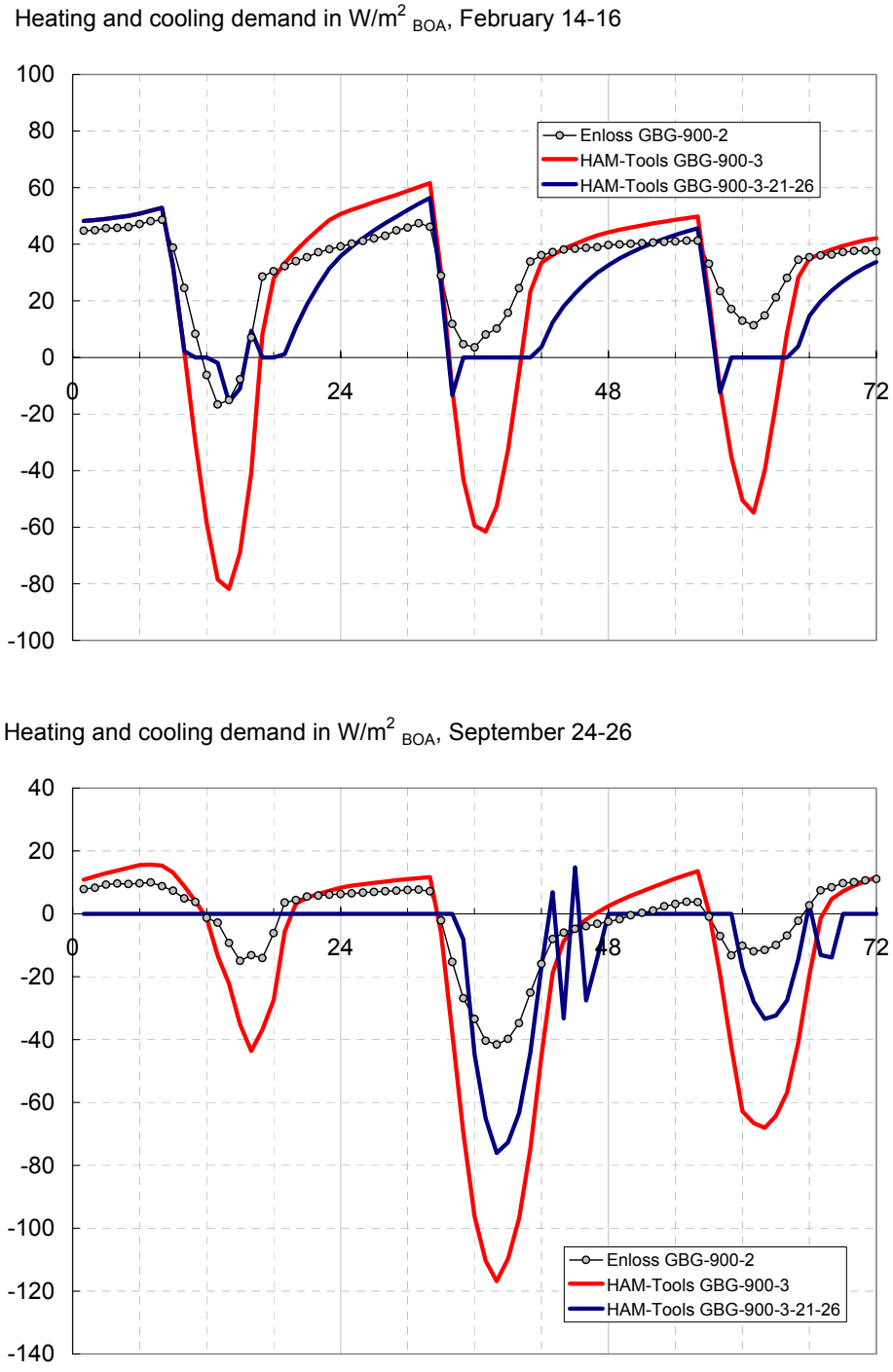

Figure 12 Hourly heating / cooling energy demands for Case 3 with two different heating / cooling set point temperatures: 21/21 °C and 21/26 °C (GBG-900). Enloss results for Case 2 are given as the reference.

7.3 Energy consumption when moisture is taken into account

This exercise aims to show to what extent the presence of moisture in the air and the construction elements can influence the energy consumption. The Case 2 is concerned, e.g. the thermal problem with solar radiation gains through windows which is described in section 5.2. The case is calculated under the following assumptions:

- The surface heat transfer coefficient are constant and equal to those proposed by the BESTEST (see section 6.3).
- The surface vapour transfer coefficients are constant and equal to 2e-8 s/m for both internal and external surfaces.
- The roof is vapour-tight on top, e.g there is no moisture exchange between the roof and the outdoor air.
- The floor is vapour-tight on internal side, e.g. there is no moisture exchange between the floor and the interior air. This is valid for both the lightweight and the heavyweight house.
- For the lightweight case, there is a vapour barrier between the plaster board and the insulation. Due to the barrier, only the plaster boards in the walls and the roof participate in moisture transfer with the indoor air.
- For the heavyweight case, the vapour barrier is placed only in the roof and not in the walls. Thus, the moisture content in the heavyweight (concrete) wall is influenced by the moisture transfer from both the outdoor and the indoor air.
- Heat losses due to ventilation are based on the difference in enthalpy between the outdoor and the indoor air. This means that the air density is also variable due to the variations in temperature and moisture content, which is a difference from all previous cases where it has been kept constant and equal to 1.2 kg/m^3 (see section 4.2.3).

HAM-Tools results for the Case 2-R-BT and Case 2-R-BT-HAM, e.g. without and with moisture calculations are shown in Table 14 and Figures 14 and 15. Generally, the influence of moisture transfer between the outdoor-indoor air and indoor air-internal walls is very small in case of the lightweight house; it is larger for the heavyweight house but still within reasonable limits.

It should be noted that the moisture transfer in these tests occurs only in vapour phase. The indoor air relative humidity is variable but within the comfort limits (see Figure 13) so there is no need for drying or humidification of the air. However, in buildings with higher internal moisture load during the day, due to for example people working inside the building, the indoor air relative humidity must be limited. This is normally done by drying of the supply air before it comes in into the building. The drying of air produces significant cooling load that must be taken into account with calculations.

Table 14 HAM-Tools results

Unit: kWh/m_{BOA}^2	GBG-600-2-R-BT		GBG-900-2-R-BT	
	no moisture calculations	with moisture calculations	no moisture calculations	with moisture calculations
Losses: windows	49.2	49.2	49.2	49.1
walls	73.9	73.5	59.4	68.3
roof	32.7	32.4	32.7	31.5
Floor	1.8	1.7	0.3	0.3
Ventilation	55.1	58.8	55.1	58.8
Sum losses	212.7	215.6	196.7	208.0
Direct solar gains	155.1	155.7	155.1	155.7
Internal gains	42.0	41.7	42.0	41.7
Heating demand	162.2	164.4	137.8	148.0
Cooling demand	96.7	95.1	72.7	67.0

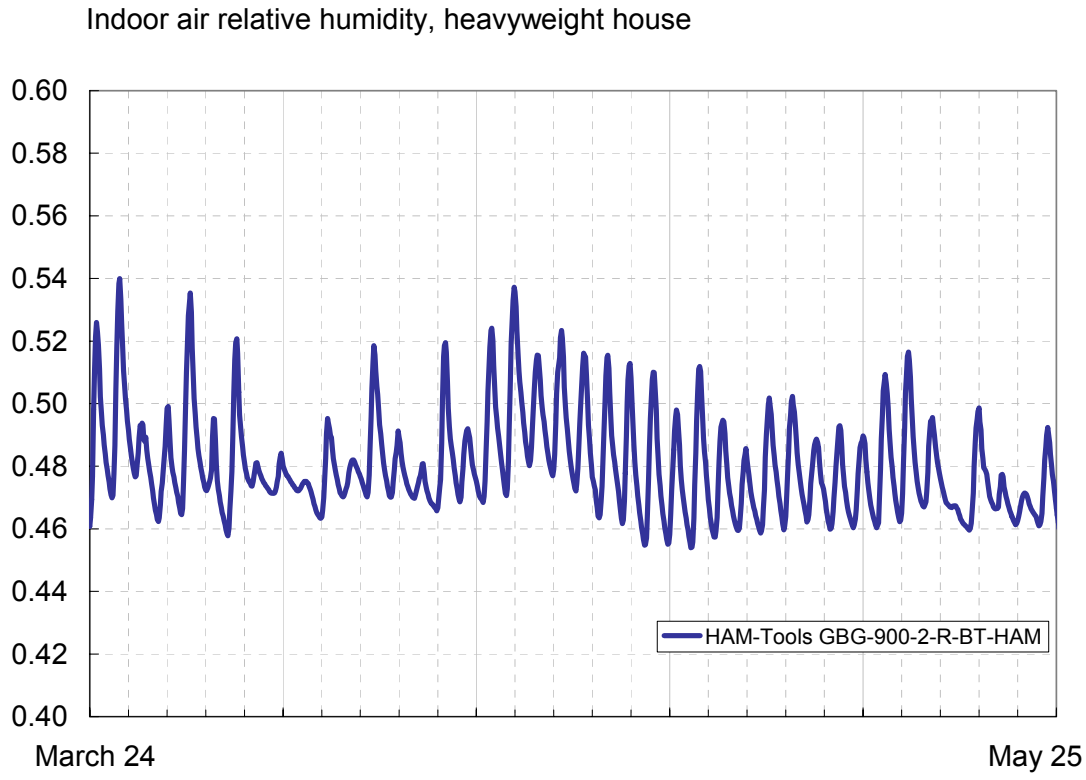

Figure 13 Indoor air relative humidity for the Case 2R-BT-HAM.

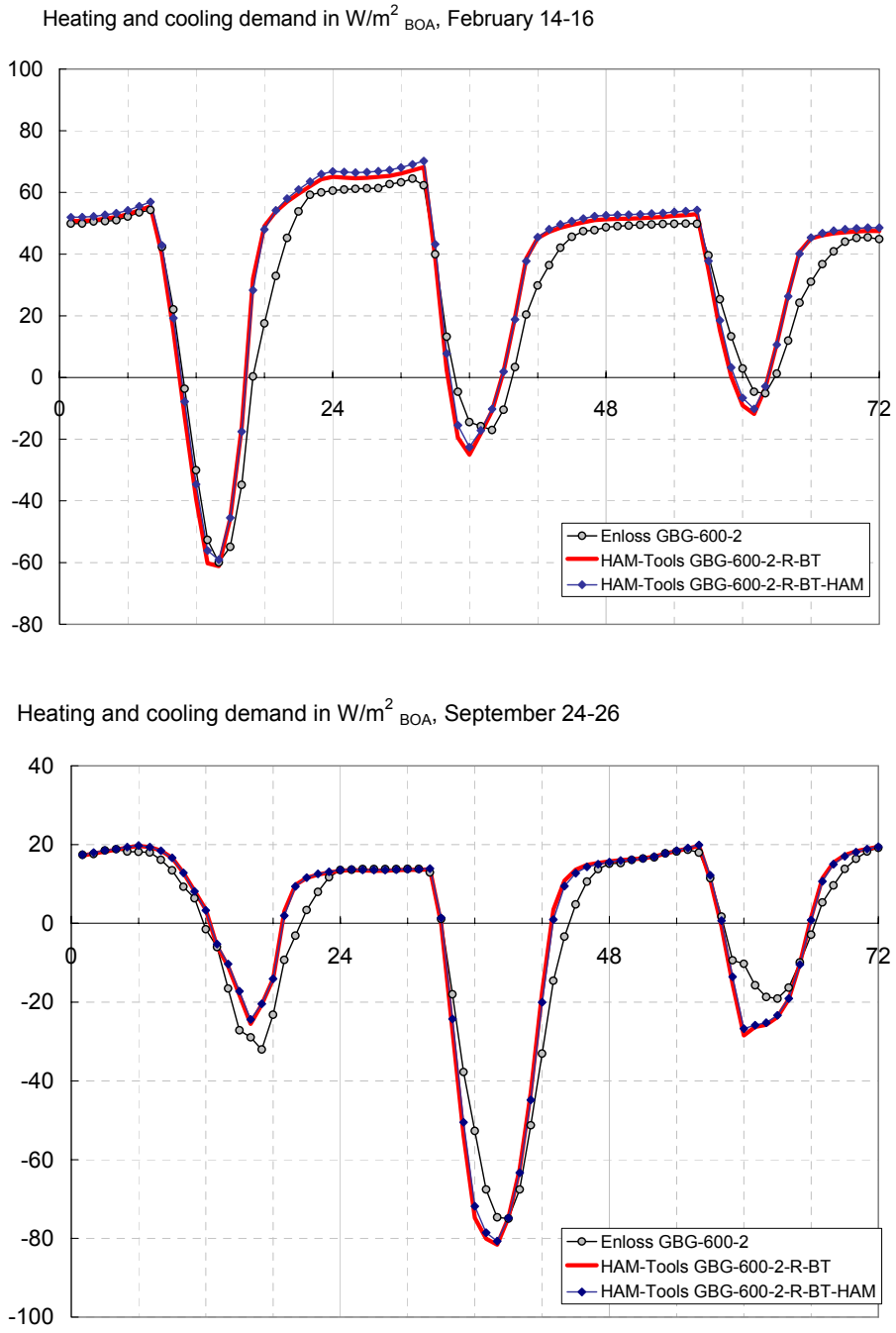

Figure 14 Hourly heating / cooling energy demands for Case GBG-600-2-R when the moisture load is taken into account. The HAM-Tools solution with moisture calculations is denoted with 2-R-BT-HAM. The HAM-Tools solution without moisture load is 2-R-BT. The BESTEST model for the heat transfer coefficients is used for the HAM-Tools solutions. Enloss results for Case GBG-600-2 are given as the reference.

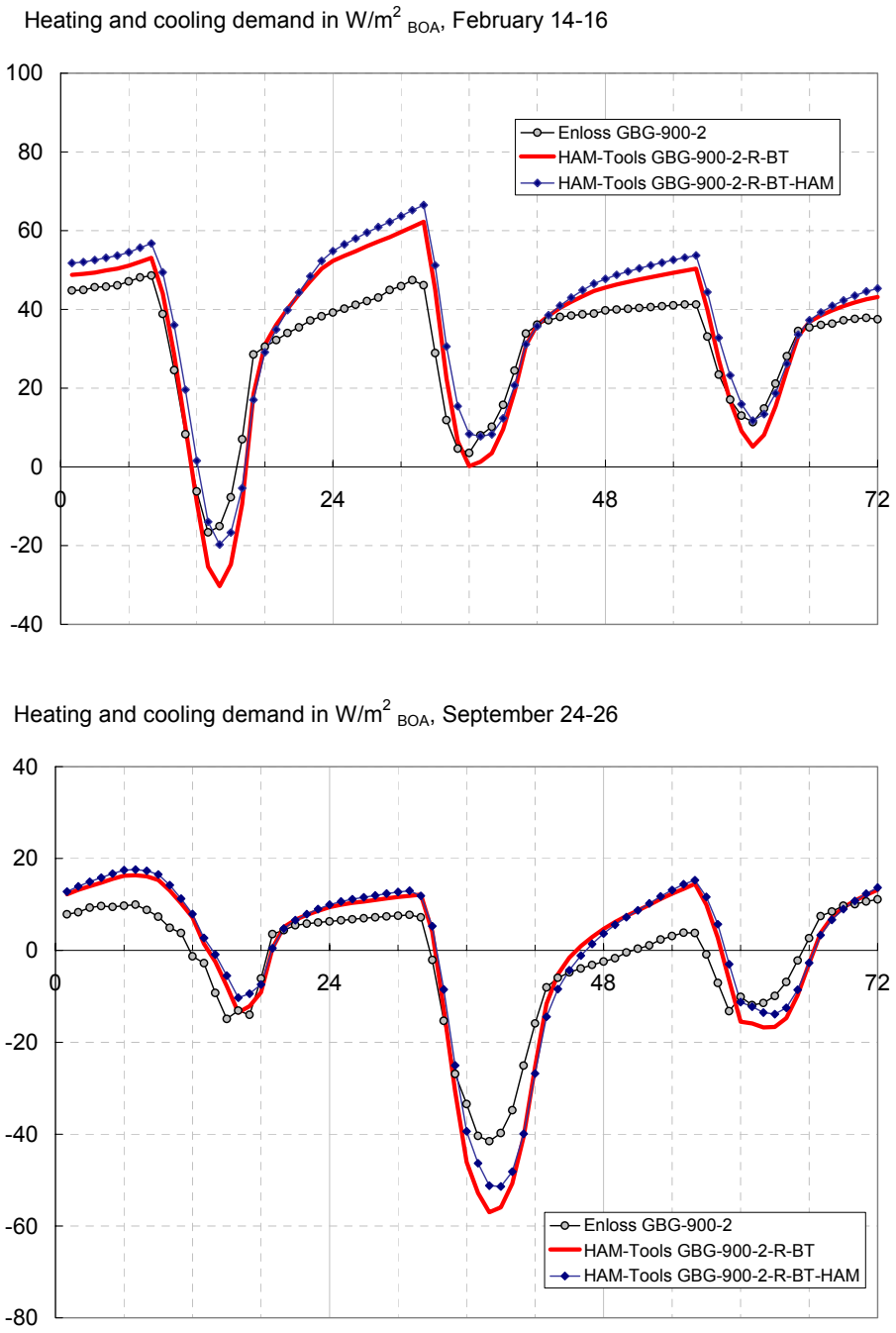

Figure 15 Hourly heating / cooling energy demands for Case GBG-900-2-R when the moisture load is taken into account. The HAM-Tools solution with moisture calculations is denoted with 2-R-BT-HAM. The HAM-Tools solution without moisture load is 2-R-BT. The BESTEST model for the heat transfer coefficients is used for the HAM-Tools solutions. Enloss results for Case GBG-900-2 are given as the reference.

8 CONCLUSIONS

The ability of Enloss to predict energy consumption of buildings was tested using the test suite which included two buildings of low and high mass construction, with mechanical ventilation, internal heat gains and solar heat gains through windows. The annual and the hourly heating and cooling demands predicted by Enloss were compared to the results of the benchmark program HAM-Tools. Based on the comparison, the agreement between the programs was very good and the largest difference in predicted annual heat consumption was 11 %.

It was found that the cause for the differences between the programs was the treatment of the solar heat gains through windows. The Enloss model used for the smoothing (weighting) of the net heat input was shown to be approximate when it was applied for the smoothing of the solar gains input. However, the Enloss procedure could be readily improved by using detailed weighting method for the solar gains. The one that was tested here was based on the theory of Dynamical Thermal Networks.

Beside these, the following Enloss models / interests were discussed with respect what was commonly used in Building Physics:

- model for the surface heat transfer coefficients
- significance of the solar irradiation on facades
- two-level thermostat control strategies
- energy consumption when the moisture transfer is taken into account

From the energy savings point of view, the first and the last topic, i.e. the model for the surface heat transfer coefficients and the effects of moisture storage in walls were shown to be of minor importance. The latter did not enclose drying of the in-built moisture or air humidification. However, the second and the third topic might be of further interest. The heat gains due to the solar irradiation on facades had some positive effects on energy savings, but the prime effect was on the increment of the cooling load. It was also shown that these effects should be considered together with the two-level thermostat control strategies, which approved variation of indoor air temperature between the thermostat set points. The variable indoor air temperature was crucial for the extra heat storage in the building construction, and based on that for the dampening of peaks in heating / cooling demand.

9 REFERENCES

1. EN ISO 13790. Thermal performance of buildings – Calculation of energy use for space heating. European Committee for standardization. Brussels, Belgium.

2. IEA International Energy Agency 1995. Building Energy Simulation Test (BESTEST) and Diagnostic Method. National Renewable Energy Laboratory, Golden, Colorado.

3. Judkoff, R., Neymark, J. 1995. International Energy Agency. Building Energy Simulation Test (BESTEST) and Diagnostic Method. National Renewable Energy Laboratory. Golden. Colorado.

4. Taesler, R., Andersson, C. & Nord, M., (in press). Optimizing energy efficiency and indoor climate by forecast control of heating systems and energy management in buildings. Report RMK 107. Norrköping: SMHI

5. Taesler, R. 1986. Climate, buildings and energy exchange – an integrated approach. Tekniska meddelanden Nr 297. KTH, Stockholm.

6. Sanders, C. 1996. IAE Annex 24, Final Report, Volume 2, Environmental conditions. K.U.Leuven, Belgium: Laboratorium Bouwfysica, Departement Burgerlijke Bouwkunde.

7. Sasic Kalagasidis, A. 2004. HAM-Tools. An integrated simulation tool for Heat, Air and Moisture transfer analyses in Building Physics. Doctoral thesis. Chalmers University of Technology, Gothenburg, Sweden. ISBN 91-7291-439-4. Computer program is available for free downloading on www.ibpt.org.

8. Sasic Kalagasidis, A. (in press). HAM-Tools testing with ANSI/ASHRAE Standard 140-2001 (BESTEST).

9. Wentzel, E-L. 2003. Application of the theory of dynamic thermal networks for energy balance of a building with three-dimensional heat conduction. Research in Building Physics. Netherlands: Balkema.

Appendix 1: Climate specifications

The weather parameters, which are based on data recorded by SMHI during 1991 at Landvetter station near Gothenburg, are summarized in Table below.

Table A1.1 Summary of climate conditions

Weather type	Mild winters and summers, often cloudy
Weather format	IBPT format
Latitude	57.67
Longitude	12.30
Altitude	154 m
Time zone	+1 east
Ground reflectivity	0.2
Site	Flat, no obstacles
Ground temperature	8 ^{o}C but 10^{o}C used in calculations
Mean annual dry-bulb temperature	7.0 ^{o}C
Minimum annual dry-bulb temperature	-14.9 ^{o}C
Maximum annual dry-bulb temperature	30.4^{o}C
Mean annual wind speed	4.2 m/s
Maximum annual wind speed	13.0 m/s
Mean annual relative humidity	80 %
Global horizontal solar radiation	961.0 kWh/m^2 year
Direct normal solar radiation	943 3 kWh/m^2 year
Diffuse horizontal solar radiation	512.7 kWh/m^2 year

Hourly variations in outdoor air temperature, global radiation on horizontal surface and wind speed are illustrated in Figure A1.1. The two characteristic periods are concerned: firstly, the coldest days in the year, February 14-16, and secondly, half-cloudy days in autumn (September 24-26) with high wind speed and moderate outdoor temperature.

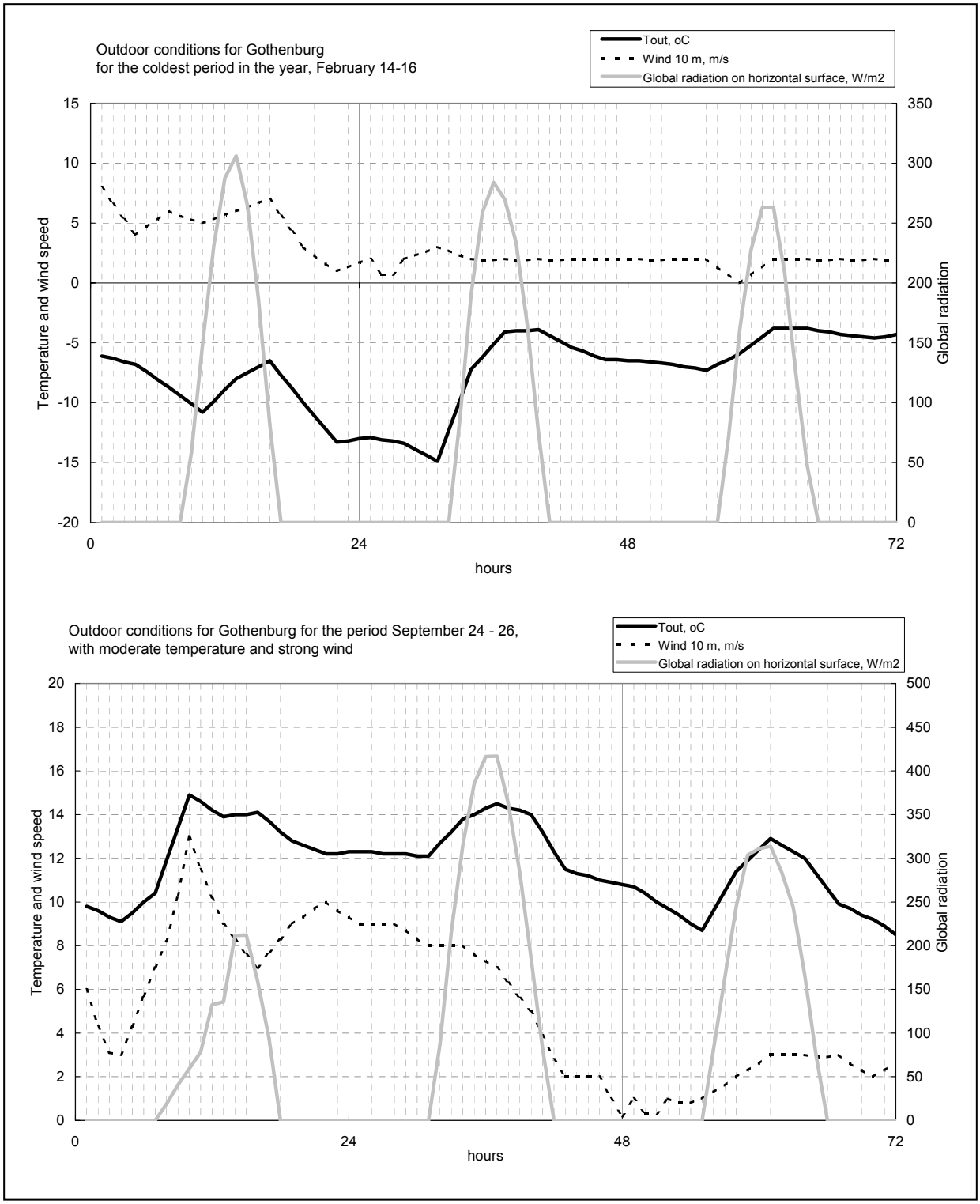

Figure A1.1 Hourly values of outdoor air temperature, global radiation on horizontal surface and wind speed for the two characteristic periods: February 14-16 when the lowest temperature occurs and September 24-26 with moderate climate and high wind speed.

Appendix 2: Determination of the thermal time constant

The thermal time constant represents a characteristic time for a temperature change in a building. If, for example, the heating system is turned off, the indoor air temperature declines towards the (constant) outdoor temperature within the time defined by the time constant. The time constant is calculated as the ratio between the volumetric heat capacity of inner layers of the building (see Figure A2.1) and the heat conductance of the building envelope.

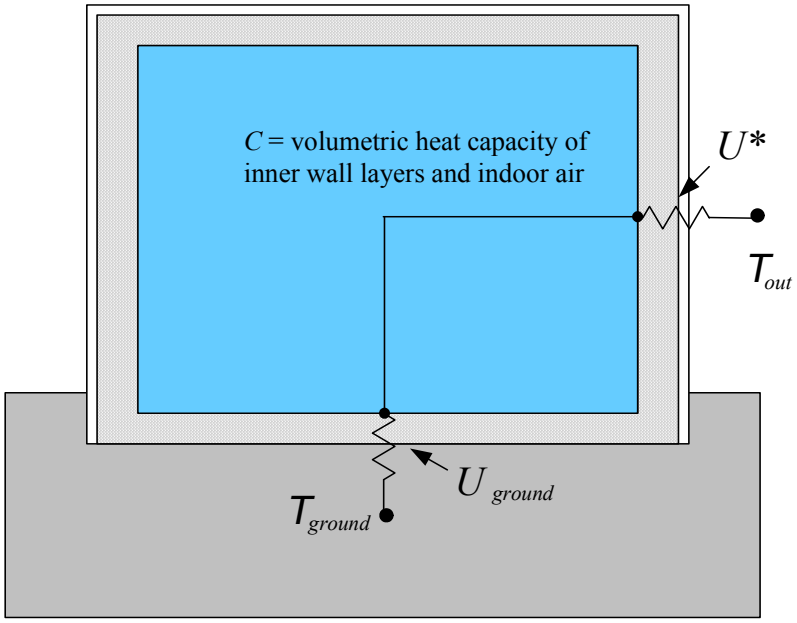

Figure A2.1 The model for the determination of the thermal time.

Assuming that the heat flow through insulated parts of the building is the steady-state one, the energy balance equation for the building reads:

$$C \cdot \frac{dT_{in}(t)}{dt} = K \cdot \left(T_{out}(t) - T_{in}(t)\right) + K_{ground} \cdot (T_{ground} - T_{in}(t)) \quad \text{(A2.1)}$$

where:

$C = C_{constr} + \rho_{air} c_{p,air} V$ is the volumetric heat capacity of air and internal wall layers,

$K = \sum_i A_i \cdot U_i^* + n \cdot \frac{\rho_{air} c_{p,air} V}{3600}$ is the heat conductance or the heat loss factor of the building, W/K. U^* is the thermal conductivity of layers which are not enclosed in C. The formula refers only to external surfaces (exposed to outdoor air).

$K_{ground} = A_{floor} \cdot U_{floor}^*$ is the heat loss factor of the floor, W/K,

Equation A2.1 can be rearranged in the following way:

$$\frac{C}{K}\cdot\frac{dT_{in}(t)}{dt}+(1+\frac{K_{ground}}{K})T_{in}(t)=T_{out}(t)+\frac{K_{ground}}{K}\cdot T_{ground} \quad \text{(A2.2)}$$

and simplified into:

$$\frac{dT_{in}(t)}{dt}+\left(\frac{1}{\tau}+\frac{1}{\tau_{ground}}\right)\cdot T_{in}(t)=\frac{1}{\tau}\cdot\left(T_{out}(t)+\frac{\tau}{\tau_{ground}}\cdot T_{ground}\right) \quad \text{(A2.3)}$$

where

$\tau=\frac{C}{K}$ is the time constant of the building

$\tau_{ground}=\frac{C}{K_{ground}}$ is the time constant of the floor

Equivalent time constant reads:

$$\frac{1}{\tau_{ekv}}=\frac{1}{\tau}+\frac{1}{\tau_{ground}}$$

or

$$\tau_{ekv}=\frac{1}{\frac{K}{C}+\frac{K_{ground}}{C}}=\frac{C}{K+K_{ground}}$$

which means that the same results will be obtained if the ground heat loss factor is enclosed in equation for the heat loss factor through the external surfaces, e.g.:

$$K=\sum_i A_i\cdot U_i^*+n\cdot\frac{\rho_{air}c_{p,air}V}{3600}+K_{ground}$$

This model is applied in the MathCad calculations that follows.

Building time constant for the SMHI model house according to EN ISO 13790:2004

Air data: specific heat capacity and density

$c_{pa} := 1000 \quad \frac{J}{kgK} \qquad \rho_a := 1.2 \quad \frac{kg}{m^3}$

Room geometry

height: $h := 2.7 \quad m$

areas: $A_{walls} := 63.6 \quad A_{floor} := 48 \quad A_{roof} := 48 \quad A_{window} := 12 \quad m^2$

volume: $V := A_{floor} \cdot h \quad V = 129.6 \quad m^3$

ventilation airflow rate: $n_v := 0.5$ U value for window (from air to air): $U := 3 \quad \frac{W}{m^2K}$

Heat transfer coefficients (mean values)

mean wind speed at 10 m height: $w_{10} := 4.2 \quad \frac{m}{s}$

mean wind speed at 2.7 m height: $w_r := 0.709 \cdot 4.2 \quad w_r = 2.978 \quad \frac{m}{s}$

mean outdoor temperature: $T_{out} := 273.15 + 7 \quad T_{out} = 280.15 \quad C$

mean indoor temperature: $T_{in} := 273.15 + 21 \quad T_{in} = 294.15 \quad C$

characteristic length (mean of the house width and length): $D := \frac{8 + 6}{2} \quad D = 7 \quad m$

mean heat transfer coefficient on external side: $\alpha_{out} := 6.4 \cdot \frac{w_r^{0.6}}{D^{0.4}} + \frac{20.8}{10^8} \cdot T_{out}^3$

$\alpha_{out} = 10.229 \quad \frac{W}{m^2K}$

mean heat transfer coefficient on internal side: $\alpha_{in} := \frac{20.8}{10^8} \cdot T_{in}^3$

$\alpha_{in} = 5.294 \quad \frac{W}{m^2K}$

Light-weight case (BESTEST 600)

Wall data (from Table 1)

plasterboard:	$d_{w1} := 0.012$	$c_{ppla} := 840$	$\rho_{pla} := 950$	$\lambda_{pla} := 0.16$
insulation:	$d_{w2} := 0.066$	$c_{pins} := 840$	$\rho_{ins} := 12$	$\lambda_{ins} := 0.04$
wood:	$d_{w3} := 0.009$	$c_{pwoo} := 900$	$\rho_{woo} := 530$	$\lambda_{woo} := 0.14$

Roof data

plasterboard:	$d_{r1} := 0.010$
insulation:	$d_{r2} := 0.1118$
wood:	$d_{r3} := 0.019$

Floor data

flooring:	$d_{f1} := 0.025$	$c_{pflo} := 1200$	$\rho_{flo} := 650$	$\lambda_{flo} := 0.14$
insulation:	$d_{f2} := 1.003$			

Assuming that all internal layers up to the insulation have the same temperature as indoor air, and neglecting the heat losses through the ground, the time constant for the house is calculated according:

$$C_{light} := d_{w1} \cdot c_{ppla} \cdot \rho_{pla} \cdot A_{walls} + d_{r1} \cdot c_{ppla} \cdot \rho_{pla} \cdot A_{roof} + d_{f1} \cdot c_{pflo} \cdot \rho_{flo} \cdot A_{floor} + c_{pa} \cdot \rho_a \cdot V$$

$$H_{light} := \frac{A_{walls}}{\frac{d_{w2}}{\lambda_{ins}} + \frac{d_{w3}}{\lambda_{woo}} + \frac{1}{\alpha_{out}}} + \frac{A_{roof}}{\frac{d_{r2}}{\lambda_{ins}} + \frac{d_{r3}}{\lambda_{woo}} + \frac{1}{\alpha_{out}}} + \frac{A_{floor}}{\frac{d_{f2}}{\lambda_{flo}} + \frac{1}{\alpha_{out}}} + U \cdot A_{window}$$

$$H_{light\_nv} := H_{light} + \frac{n_v \cdot c_{pa} \cdot \rho_a \cdot V}{3600}$$

$C_{light} = 2.084 \times 10^6 \quad \frac{J}{K}$ $\qquad H_{light} = 93.558 \quad W$

$H_{light\_nv} = 115.158$

with zero ventilation airflow rate (nv=0 ach):

$$\tau_{light} := \frac{C_{light}}{H_{light}}$$

$$\frac{\tau_{light}}{3600} = 6.186 \quad h$$

with 0.5 ach

$$\tau_{light\_nv} := \frac{C_{light}}{H_{light\_nv}}$$

$$\frac{\tau_{light\_nv}}{3600} = 5.026 \quad h$$

Heavy-weight case (BESTEST 900)

Wall data (from Table 2):

concrete:	$d_{w1} := 0.100$	$c_{pcon} := 1000$	$\rho_{con} := 1400$	$\lambda_{con} := 0.51$
insulation:	$d_{w2} := 0.0615$	$c_{pins} := 1400$	$\rho_{ins} := 10$	$\lambda_{ins} := 0.04$
wood:	$d_{w3} := 0.009$	$c_{pwoo} := 900$	$\rho_{woo} := 530$	$\lambda_{woo} := 0.14$

Roof data

plasterboard:	$d_{r1} := 0.010$
insulation:	$d_{r2} := 0.1118$
wood:	$d_{r3} := 0.019$

Floor data

flooring:	$d_{f1} := 0.080$	$c_{pflo} := 1000$	$\rho_{flo} := 1400$	$\lambda_{flo} := 1.13$
insulation:	$d_{f2} := 1.007$			

$$C_{heavy} := d_{w1} \cdot c_{pcon} \cdot \rho_{con} \cdot A_{walls} + d_{r1} \cdot c_{ppla} \cdot \rho_{pla} \cdot A_{roof} + d_{f1} \cdot c_{pflo} \cdot \rho_{flo} \cdot A_{floor} + c_{pa} \cdot \rho_a \cdot V$$

$$H_{heavy} := \frac{A_{walls}}{\frac{d_{w2}}{\lambda_{ins}} + \frac{d_{w3}}{\lambda_{woo}} + \frac{1}{\alpha_{out}}} + \frac{A_{roof}}{\frac{d_{r2}}{\lambda_{ins}} + \frac{d_{r3}}{\lambda_{woo}} + \frac{1}{\alpha_{out}}} + \frac{A_{floor}}{\frac{d_{f2}}{\lambda_{flo}} + \frac{1}{\alpha_{out}}} + U \cdot A_{window}$$

$$H_{heavy\_nv} := H_{heavy} + \frac{n_v \cdot c_{pa} \cdot \rho_a \cdot V}{3600}$$

$C_{heavy} = 1.482 \times 10^7 \quad \frac{J}{K} \qquad H_{heavy} = 137.809 \quad W$

$H_{heavy\_nv} = 159.409$

<u>with zero ventilation airflow rate (nv=0 ach)</u>:

$$\tau_{heavy} := \frac{C_{heavy}}{H_{heavy}}$$

$$\frac{\tau_{heavy}}{3600} = 29.869 \quad h$$

<u>with 0.5 ach</u>

$$\tau_{heavy\_nv} := \frac{C_{heavy}}{H_{heavy\_nv}}$$

$$\frac{\tau_{heavy\_nv}}{3600} = 25.822 \quad h$$

Appendix 3: Wind velocity at the sight

The Enloss model for wind velocity at different heights on different sites is based on the logarithmic profile model:

$$w_z = \frac{w^*}{\kappa} \ln\left(\frac{z}{z_0}\right) \quad \text{(A3.1)}$$

where w^* is the friction velocity, κ is the Karman coefficient depending on the terrain type and z_0 is the roughness length (see for example Sanders, 1996).

Firstly, the wind velocity at 300 m height is deduced from the one measured at 10 m height at the meteorological station:

$$w_{300} = w_{10} \cdot \frac{\ln(300/z_{01})}{\ln(10/z_{01})} \quad \text{(A3.2)}$$

It is assumed here that obstacles at the ground level do not influence the wind velocity at 300 m height. Secondly, the value w_{300} is used to calculate the velocity at other heights (h) and possibly other terrains (in terms of the roughness factor):

$$w_h = w_{300} \cdot \frac{\ln(h/z_{02})}{\ln(300/z_{02})} \quad \text{(A3.3)}$$

In the test presented, the value of $z_{01} = 0.02$ is used for w_{300}:

$$w_{300} = w_{10} \cdot 1.547$$

and $z_{02} = 0.05$ for the velocity at 2.7 m height (the height of the test house):

$$w_{2.7} = w_{300} \cdot 0.4585 = w_{10} \cdot 0.709$$

Appendix 4: Solar gains as the radiative heat source

(based on the theory of dynamical thermal networks)

The following equations present the energy balance model of the house, where the solar gains are introduced as the radiative source. For the sake of simplicity, the heat transfer coefficients on external and internal side of the construction are set constant and equal to the standard values of 25 W/m^{2}K and 7.7 W/m^{2}K respectively. This simplification excludes effects of variable outdoor air temperature and wind speed on the exterior heat transfer coefficient; furthermore, it is convenient to use standard values whenever study on another parameter is to be performed. It is also assumed that each internal surface gets the same amount of net solar energy, i.e. that the incoming solar gains are uniformly distributed.

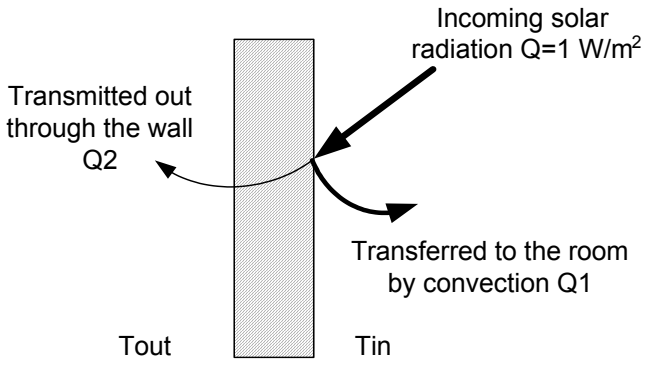

Figure A4.1 The solar energy distribution in the radiative model

Hypothesis

The incoming (net) solar radiation hits and warms a surface. One part is transferred back to the room by convection[3], Q_1, while the other part is transmitted through the wall, Q_2. Both parts appear as heat sources.

$$Q(t) = Q_1(t) + Q_2(t) \quad \text{(A4.1)}$$

$$Q_1(t) = \alpha_{in}\left[T_{surf}(t) - T_{in}\right] \quad \text{(A4.2)}$$

$$Q_2(t) = K^*\left[T_{surf}(t) - T_{out}\right] \quad \text{(A4.3)}$$

where

[3] This is also a simplification, since this part of the heat is transfered to the room by convection and long-wave radiation, while a part of it is reflected to other surfaces.

$K^* = \dfrac{1}{\dfrac{1}{\alpha_{out}} + K}$ and K is the wall conductivity.

For T_{out}=T_{in}=0 and in a steady-state:

$$\frac{Q_2}{Q_1} = \frac{K^*}{\alpha_{in}}$$

(A4.4)

e.g., the less the wall is insulated, the more heat will be lost by transmittion.

For the test house, $\alpha_{in} = 7.6$ W/m^{2}K (standard value) and $K^* = 0.6$ W/m^{2}K, turns out that about 8 % of the incoming solar radiation will be transferred through the wall by transmittion:

$$Q_2 \approx 0.08 \cdot Q$$

(A4.5)

The dynamics of this process for the lightweight and the heavyweight wall are illustrated in Figure A4.2.

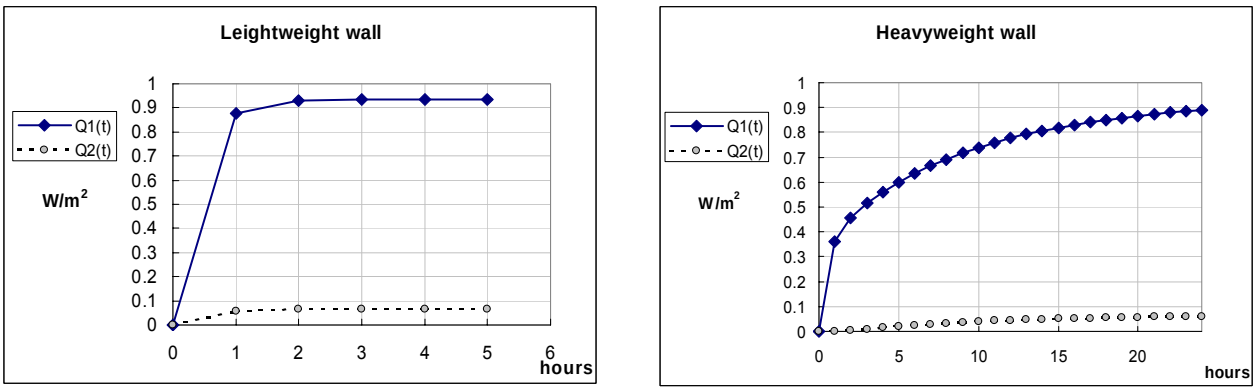

Figure A4.2 Thermal response of the lightweight and the heavyweight wall on internal radiative heat source

For the lightweight wall, the most of the incoming solar radiation is transferred to the indoor air by convection within the first two hours, while it takes much longer time, at least 10 hours, for the heavyweight wall.

The convective and transmitted part of the solar radiation are obtained as:

$$Q_1(t) = \sum_{m=1}^{M} \kappa_{sol,1}(t_0 - m \cdot \Delta t) \cdot Q(m \cdot \Delta t) \cdot \Delta t$$

(A4.6)

$$Q_2(t) = \sum_{m=1}^{M} \kappa_{sol,2}(t_0 - m \cdot \Delta t) \cdot Q(m \cdot \Delta t) \cdot \Delta t$$

(A4.7)

where $\kappa_{sol,1}$ and $\kappa_{sol,2}$ are weighting factors, calculated using the theory of dynamical thermal networks (Wentzel, 2005):

$$\kappa_{sol,1} = \frac{1}{\alpha_{in}} \frac{dQ_1(t)}{dt}$$

(A4.8)

$$\kappa_{sol,2} = \frac{1}{K^*} \frac{dQ_2(t)}{dt}$$

(A4.9)

The magnitude and the time distribution of the solar weighting factors for the lightweight and the heavyweight walls are shown in Figure A4.3. The effect of the incoming solar radiation as the radiative heat source is shown in Figure A4.4. Note how this effect appears later, more dampened and then prolonged in the case of the heavyweight construction compared to the lightweight one. The results are based on the above-presented method.

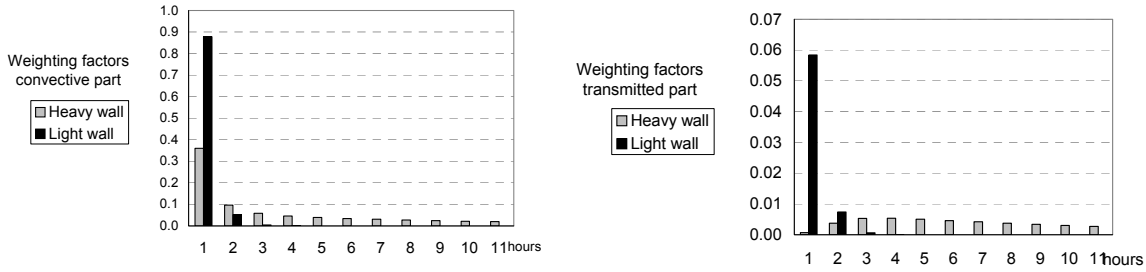

Figure A4.3 Thermal response factors (weighting factors) for solar radiation as the internal radiative heat source

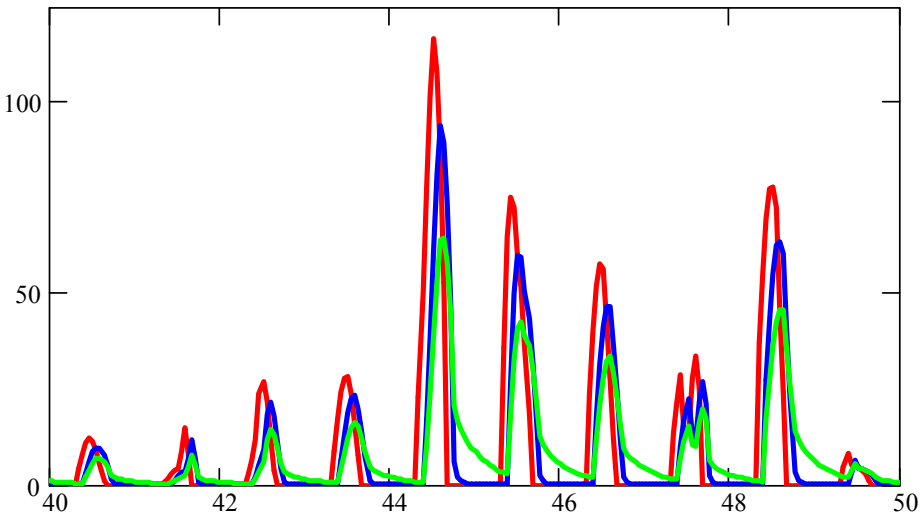

Figure A4.4 The effect of the solar radiation as the radiative heat source, calculated by the solar weighting factors: for the lightweight house (blue line) and for the heavyweight one (light green), in W/m^2 of the floor area. The total incoming radiation is shown with the red line, from the Gothenburg climate data file.

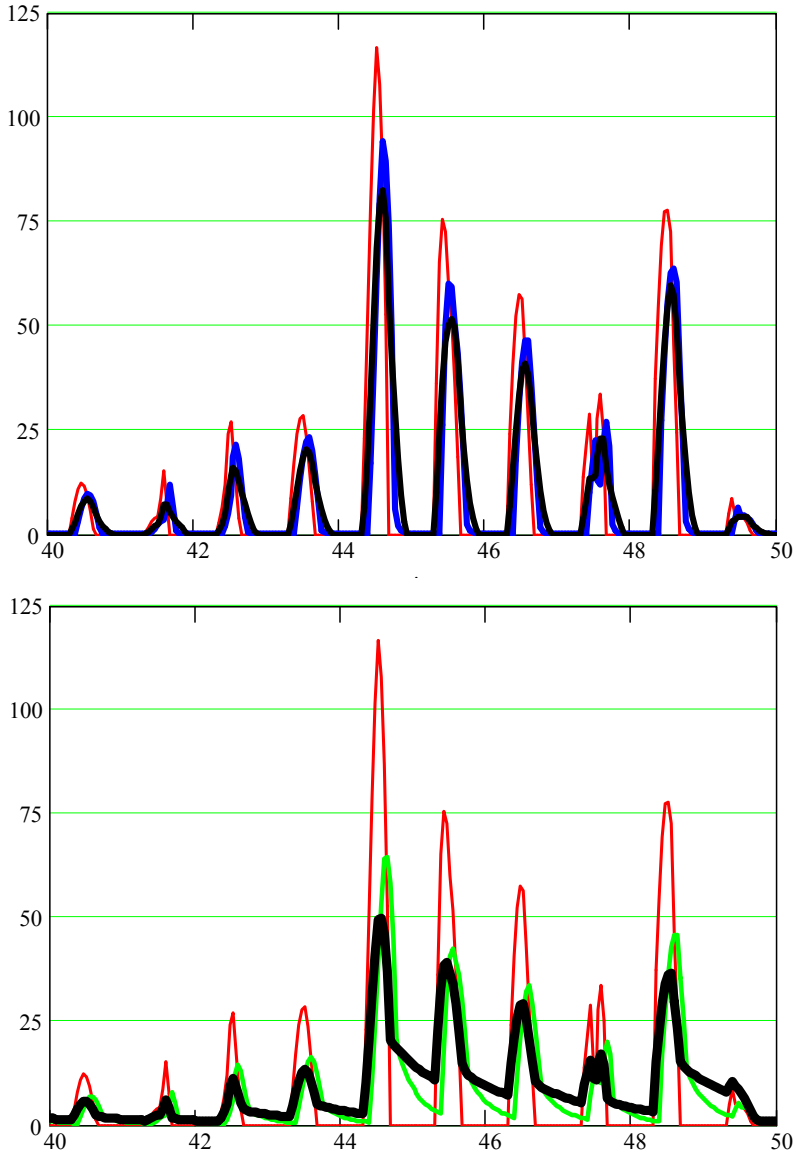

Figure A4.5 shows the same effect calculated with Enloss, for the light and the heavy construction, respectively. There is some minor difference in the case of the light construction, but noticeably different distribution is obtained for the heavy one: firstly, the effect appears earlier, in the phase with the incoming radiation, secondly, it is more dampened compared to the solution from the dynamical thermal networks, and thirdly, it has the higher effect after the sunny hours are over. Note that the total effect, i.e. when summed over the time, is the same for both methods.

As it is discussed in section 5.2.1, the difference between Enloss and HAM-Tools solutions is due to the different solar weighting factors. Using the solar weighting factors from the above-presented method (Equations A.4.7-8) in the model proposed by Equation 19 from section 5.2.1, the excellent agreement is achieved between the solutions. This is also proved in the last calculation example, which is presented in the paper that followed this testing. The paper is enclosed in Appendix 7 and the results are summarized in the table below.

Figure A4.5 The effect of the solar radiation as the radiative heat source, calculated by the solar weighting factors (blue and light green) and Enloss (black), in W/m^2 of

the floor area. The total incoming radiation is shown with the red line. The upper figure refers to the light construction, the lower to the heavy construction.

Table A4.1 Annual energy consumption of the standard-test houses with ventilation and solar radiation, in kWh/m^2 of the floor area. More details are given in Appendix 7.

Method	Lightweight house		Heavyweight house	
Enloss	175.0 Equation 14	184.5 Equation 19	146.0 Equation 14	159.1 Equation 19
HAM-Tools	185.9		165.2	

Appendix 5: Heat losses due to air-infiltration

(the ENLOSS model)

Leakage factors for the model building

The mean leakage factor $\bar{k}$ of a building is defined for the 50 Pa pressure difference and only for external surfaces (external walls and roof):

$$\bar{k} = \frac{n_{50} \cdot V}{50^{\beta} \cdot A_{external}}, \qquad \text{(A5.1)}$$

$$A_{external} = A_{ext.walls} + A_{roof}$$

where n_{50} is the air change rate per hour at 50 Pa, V = 112.7 m^3 is the volume of the house, β = 0.65 is the parameter in the airflow equation, $A_{ext.walls}$ = 123.6 m^2 is the area of external walls and A_{roof} = 48 m^2 is the roof area.

It is assumed that leakage factor of the roof $\bar{k}_{roof}$ is one half of the leakage factor of external walls $\bar{k}_{ext.walls}$:

$$k_{ext.walls} = 2 \cdot k_{roof} \qquad \text{(A5.2)}$$

$$\bar{k} = \frac{k_{ext.walls} \cdot A_{ext.walls} + k_{roof} \cdot A_{roof}}{A_{external}}$$

$$\Rightarrow \quad k_{roof} = \frac{\bar{k} \cdot A_{external}}{2A_{ext.walls} + A_{roof}} \qquad \text{(A5.3)}$$

In SBN (Swedish Building Code) 1980, second edition, Tabel 33:31, n_{50} equals to 3 h^{-1} for single family houses in open position to the wind. Using this value, the leakage factors from equations A3.1-3 are determined as $k_{ext.walls} = 0.26$ and $k_{roof} = 0.13$ (in m^3/m^{2}Pa$^{0.65}$h). The rounded values of 0.3 and 0.15 m^3/m^{2}Pa$^{0.65}$h are used in the calculations (8.3·10^{-5} and 4.2·10^{-5} m^3/m^{2}Pa$^{0.65}$s), which results in n_{50}=3.3 h^{-1}.

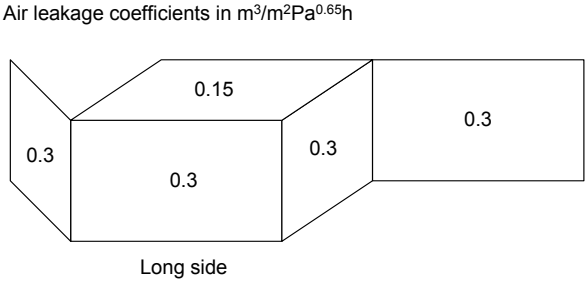

Distribution of air leakages

The ENLOSS air infiltration model is described in details in Teasler, 1986. A summary of details needed for producing a similar model in HAM-Tools / Simulink is given hereafter.

The model distinguishes windward and leeward sides of the building. Overpressure caused by the wind at the windward side will contribute to the greater air inflow in the lower part of the subjected surface, e.g. below the neutral pressure plane. Consequently, due to the under pressure, the air outflow at the leeward side will increase in the upper part of the surface. These effects are indicated by placing the neutral pressure plane at the windward side, NPP_1, above the one on the leeward side, NPP_2.

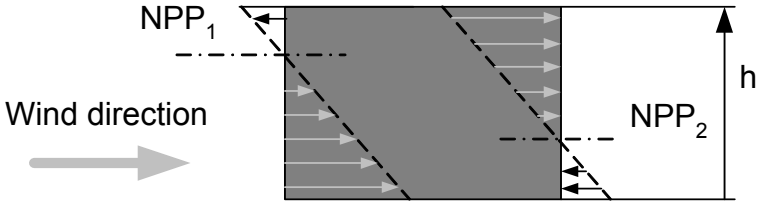

Positions of air leakages at the windward and leeward side are determined by their relative position to the NPP_1 and NPP_2 respectively. When the height (z) of the NPP is within 0 and the wall height h, two leakage paths are concerned: below the NPP, which are grouped at the height $0.5z$ and above the NPP at the height $z+0.5(h-z)$, as shown in the next figure.

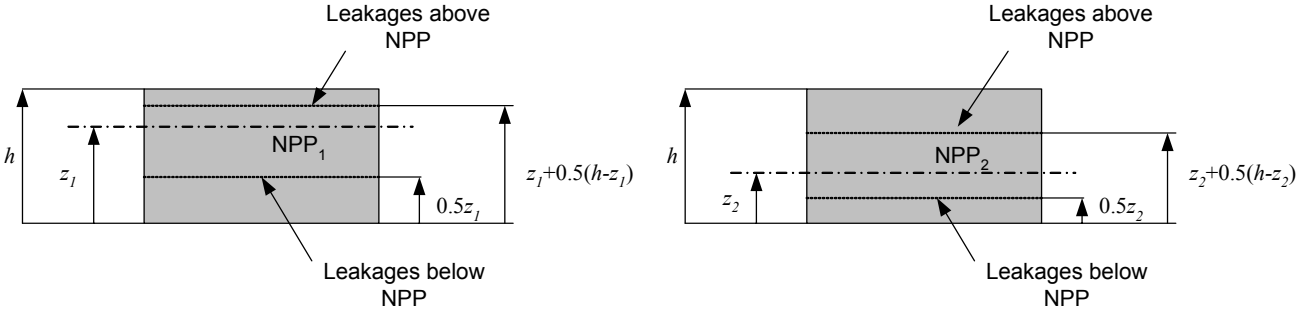

Leakages on the walls at the side of the windward wall, to be called here "the side walls", are positioned in the middle of the wall height:

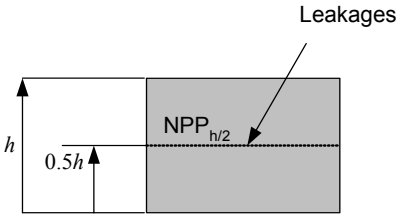

Airflow direction: the flow is considered positive (i.e., goes into the building) when the outdoor air temperature is lower than the indoor one.

When the NPP is above the wall height h, one leakage path is considered at the height z-0.5h, (see the figure above). When the NPP is below the ground, one leakage path is considered at the height $-z$+0.5h.

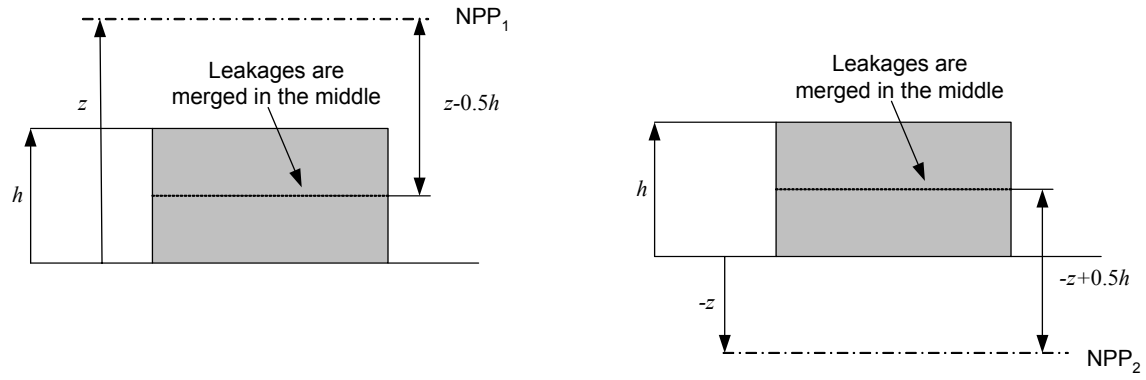

Windward side Leeward side

Table A5.1 Summary of applied heights and areas, when 0 < NPP < h

Surface	Surface indices *(i, j)*	Height of NPP *z(i,j)*	Area $A_{i,j}$	k_i ($m^3/m^2Pa^{0.65}h$)	Aiflow direction
Windward wall, lower part	(1,1)	$0.5 \cdot z_1$	$8 \cdot z_1$	0.3	+
Windward wall, upper part	(1,2)	$z_1 + 0.5 \cdot (h - z_1)$	$8 \cdot (z_1 + 0.5 \cdot (h - z_1))$	0.3	-
Leeward wall, lower part	(2,1)	$0.5 \cdot z_1$	$8 \cdot z_1$	0.3	+
Leeward wall, upper part	(2,2)	$z_1 + 0.5 \cdot (h - z_1)$	$8 \cdot (z_1 + 0.5 \cdot (h - z_1))$	0.3	-
Side walls, whole area	(3,1) and (3,2) (4,1) and (4,2)	$0.5 \cdot h$	$6 \cdot h$	0.3	-
Roof, whole area	(5,1) and (5,2)	h	8·6	0.15	-

Table A5.2 Summary of applied heights and areas, when NPP > h and NPP < 0

Surface	(i, j)	*z(i,j)*	Area $A_{i,j}$	k_i ($m^3/m^2Pa^{0.65}h$)	Aiflow direction
Windward wall, NPP>h	(1,1) and (1,2)	$z_1 - 0.5 \cdot h$	$8 \cdot h$	0.3	+
Windward wall, NPP<0	(1,1) and (1,2)	$-z_1 + 0.5 \cdot h$	$8 \cdot h$	0.3	-
Leeward wall, NPP>h	(2,1) and (1,2)	$z_1 - 0.5 \cdot h$	$8 \cdot h$	0.3	+
Leeward wall, NPP<0	(2,1) and (1,2)	$-z_1 + 0.5 \cdot h$	$8 \cdot h$	0.3	-

Infiltration airflow rate caused by the wind

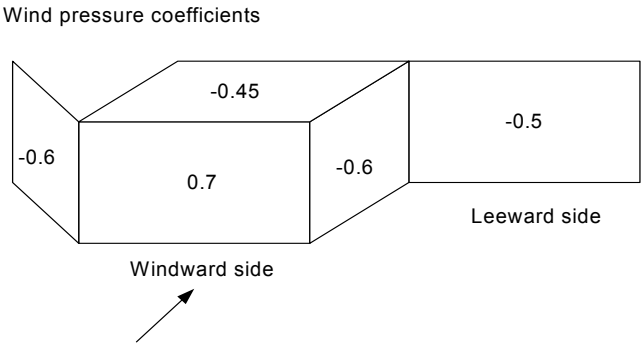

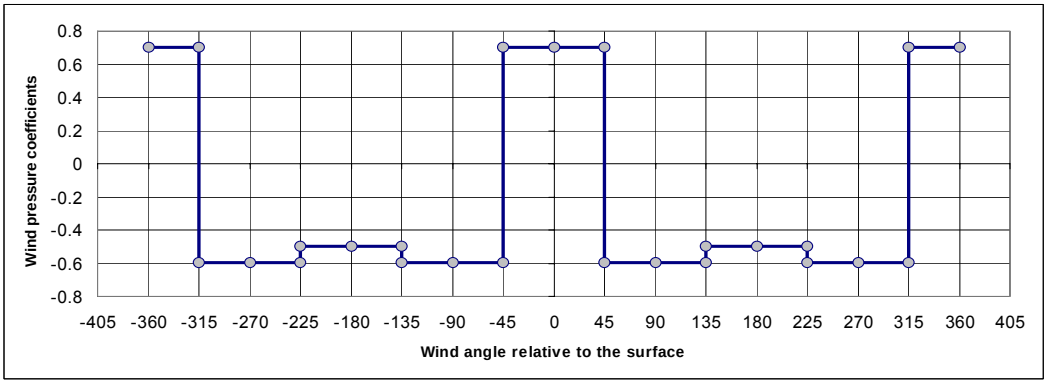

The mass airflow rate through the surface number i is given as:

$$m_i^{wind} = \rho_{air} \cdot A_i \cdot c_i \cdot \Delta P_{wind,i}^{0.65} \tag{A5.4}$$

where

$$\rho_{air} = \begin{cases} \rho_o(T_{out}) \text{ when the flow is directed into the building} \\ \rho_{in}(T_{in}) \text{ when the flow is directed out of the building} \end{cases} \tag{A5.5}$$

$$\Delta P_{wind,i} = P_{out,i} - P_{in} \tag{A5.6}$$

The total pressure in front of the surface is a sum of the static air pressure P_o= 101325 Pa and the dynamic pressure caused by the wind:

$$P_{out,i} = P_o + 0.5 \cdot \rho_o \cdot w_{2.7}^2 \tag{A5.7}$$

The vind pressure coefficients for vertical and horizontal surfaces c_i are given in the figure and the diagram above.

Infiltration airflow rate through leakages

The mass airflow rate through the leakage number i,j is given as:

$$m_{i,j}^{leakage} = \rho_{air} \cdot A_{i,j} \cdot k_i \cdot (\Delta P_{stack,i,j} + \Delta P_{wind,i})^{0.65} \tag{A5.8}$$

where ρ_{air} as in equation A5.5.

$$\Delta P_{stack,i,j} = z_{i,j} \cdot g \cdot \frac{P_o}{R}\left(\frac{1}{T_{out}^K} - \frac{1}{T_{in}^K}\right) \quad \text{(A5.9)}$$

$\Delta P_{wind,i}$ is the wind caused pressure difference from equation A5.6.

T_{out}^K, T_{in}^K are outdoor and indoor air temperatures, (K)

R = 287.015 J/kgK, the gas constant for the air

g = 9.81 m/s^2, the acceleration of the gravity

$A_{i,j}$ the surface partition as it is given in Tables A5.1 and A5.2

k_i the leakage factor, Table A5.1

The indoor air pressure P_{in} and the location of the NPP z are found iteratively from the mass airflow balance:

$$\sum_{i=1}^{5} m_i^{wind} + \sum_{i=1}^{5}\sum_{j=1}^{2} m_{i,j}^{stack} = 0 \quad \text{(A5.10)}$$

Annual heat losses due to air infiltration on the test house are estimated to be 30.9 kW/m^2 (HAM-Tools) and 31.8 kW/m^2 (Enloss). Comparison of hourly values of heat losses is shown in the figure below.

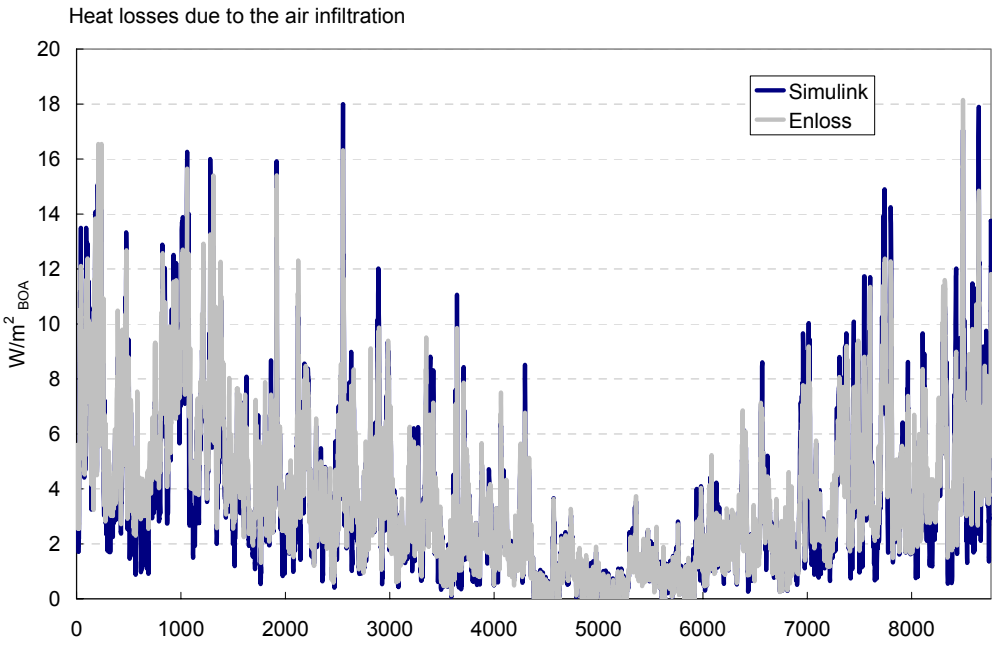

Appendix 6: The function of Venetian blinds

This chapter presents the Enloss model for the window shading coefficient *s* (see sections 3.3.3 and 4.2.4). The model is meant to simulate the use of Venetian blinds as the window shading device. Thus, the coefficient itself is called the function of Venetian blinds.

This coefficient says how much of the solar energy is transferred through the window when the shading device is used, compared to the amount transferred through the un-shaded window. Values for closed Venetian blinds regarding their position and colour are shown in Table A6.1

Table A6.1 Shading coefficients for shading with Venetian blinds. Values refer to closed blinds.

	indoor	between glass	outdoor
white	0.6	0.35	0.2
dark	0.8	0.45	0.1

The position of blinds (i.e. open, semi-open or closed) is normally correlated to the intensity of solar radiation through the window and the angle of incidence of the solar beam on the window plane. The following relation is used to describe the position of blinds:

$$s(t) = 1 - 0.65 \cdot \left(q_{sol}(t) / q_{sol,ref} \right)^{0.25} \tag{A6.1}$$

where q_{sol} is the total (global) instantaneous solar radiation intensity through all windows, $q_{sol,\,ref}$ is the maximal expected one at the south-oriented surface and t is the time.

q_{sol} is found from the following approximate relation:

$$q_{sol}(t) = \frac{A_{window}}{A_{BOA}} \cdot \tau_w \cdot I_{dir}(t) \cdot (0.125 \cdot \sin(\theta(t)) + 0.676 \cdot \cos(\theta(t))) \tag{A6.2}$$

where τ_w is the window transmittance, I_{dir} is the direct solar radiation on the south-oriented window and θ is the angle of incidence (see Figure A6.1). The expression between the parenthesis has the maximum value 0.7 when the angle of incidence equals 10.5°. Therefore, the reference solar radiation intensity is approximated as the maximal direct solar radiation intensity $I_{dir,\max}$ times 0.7:

$$q_{sol,ref} = \frac{A_{window}}{A_{BOA}} \cdot \tau_w \cdot 0.7 \cdot I_{dir,\max} \tag{A6.3}$$

It is further assumed that 85 % of the global radiation intensity refers to the direct component, while the rest is the diffuse radiation. The global radiation intensity at south-oriented surface is calculated from the following equation:

$$I_{global}(t) = 1100 \cdot e^{-0.14/\sin h(t)} (\cos(h(t)) - 0.29 \cdot \sin(h(t)) + 377 \cdot \sin(h(t)) \tag{A6.4}$$

The maximum value of I_{global} equals to 790 W/m^2 when the sun height is 30^o (see Table A6.2). The maximum is rather flat and the value of 780 W/m^2 is used to calculate the maximum direct solar radiation:

$$I_{dir,max} = 0.85 \cdot 780 = 660 \ \text{W/m}^2 \tag{A6.5}$$

Combining equations A6.1-3 and 5 the final expression for *s* reads:

$$s(t) = 1 - 0.65 \cdot \left(\frac{I_{dir}(t) \cdot (0.125 \cdot \sin(\theta(t)) + 0.676 \cdot \cos(\theta(t))}{660} \right)^{0.25}$$

Table A6.2 Global radiation intensity as a function of the sun height.

h	5	10	15	20	25	30	35	40	45	50
$I_{global,\ max}$	245	525	670	745	780	790	780	755	720	675

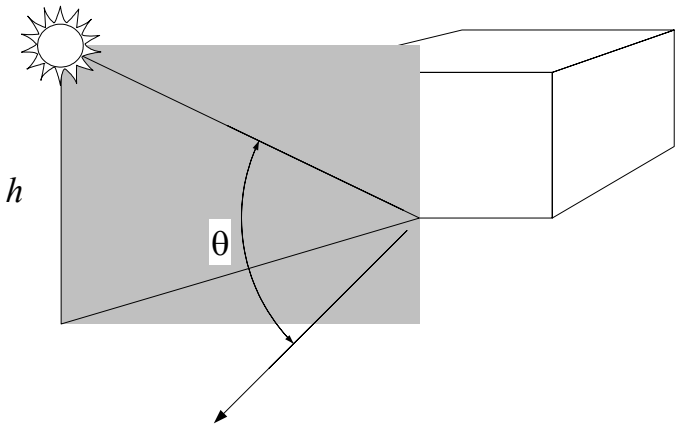

Figure A6.1 The angle of incidence and the solar height

Appendix 7: Empirical validation of the ENLOSS-model

ENLOSS-calculations of net heating demand (q_N) are validated against one year of measured hourly data from a real building. The *net heating demand* is the heat required for space heating only, not including heat for domestic hot water production.

The building is supplied with energy from a district heating system. Before March 20 2002 the heat supply from the district heating system was used for space heating only. From this date and onwards the measured heat consumption includes space heating as well as domestic hot water production. Assuming the monthly volume of hot water consumption to be approximately constant it is possible to determine with good accuracy the monthly heat requirements before and after March 2002. The net energy used for space heating is obtained by reducing the total measured energy input from the district heating system by the heat required for hot water production.

1 The Building

The building used in this evaluation is a residential house, located in Köping, Sweden (lat=59.51 long=16.01). It is a five-storey house, four of which contain flats (cf. Fig.1).

Figure A7.1. Facade of the test building, facing towards NW.
The length axis of the building is orientated SW-NE.

2 Thermal properties

The thermal properties of the building are shown in Table A7.1.

Table A7.15 Thermal properties for the building in Köping.

Layer		λ	d	U	Area
	Unit	W/m,K	m	$W/m^2,K$	m^2
Exterior wall	Facing brick	0.60	0.120		
	Gypsum board	0.22	0.009		
	Insulation	0.04	0.170		
	Gypsum board	0.22	0.013		
	Total (U_o)			0.26	1320
Ground floor	Total (U_o)			0.30	737,5
Roof	Total (U_o)			0.17	764
Windows	Total (U_o)			1.4	233

The building's thermal inertia is treated by weighting the energy consumption backwards in time. In this case the weighting period for the whole building is set to 18 hours, (time constant τ=18 h).

2.1 Geometry for the tested building

The total horizontal area of the building is 760 m^2, calculated from the outer dimensions (length and width). This value is corrected to 737.5 m^2 to account for unheated balconies.

The measured energy consumption is normalized by a heated area (BOA) 2633 m^2 as given by the owner of the house. This value does not include parts of the bottom floor but represents only the area for which rent is being paid. In the simulations the entire heated area of all the 5 floors are included, giving a heated floor area of 3208 m^2. The latter value is calculated as 87 % of the total, outer floor area of the 5 storeys.

BOA area $$A_{BOA} = 737.5 \cdot 5 \cdot 0.87 = 3208 \text{ m}^2$$

The reason is that the ENLOSS model assumes that the whole building is heated. Thus, the energy consumption is normalized to that area.

2.2 Ventilation

The house is supplied with outdoor air by a mechanical ventilation system giving a ventilation airflow rate of 0.8 ach^{-1} during daytime and 0.4 ach^{-1} during nighttime. No heat exchange takes place between exhaust and supply air.

2.3 Windows

The windows are triple-glazed. A constant transmission coefficient for solar radiation α = 0.48 is used. Shading due to Venetian blinds or other devices is taken into account as explained in appendix II.

2.4 Internal heat gains

Internal heat gains from occupants and use of electric appliances is set to 2.2 W/m^2 during day and 2.9 W/m^2 during night.

2.5 Indoor temperature

Indoor temperatures were measured once every hour continuously during the evaluation period. The average value during the heating season was + 23 ^{o}C with a standard deviation of typically 0.33 ^{o}C . Comparison of the frequencies of temperaturevalues for different hours of the day (c.f. Figure. 2) show no diurnal trend, indicating that the heating system is well adjusted.

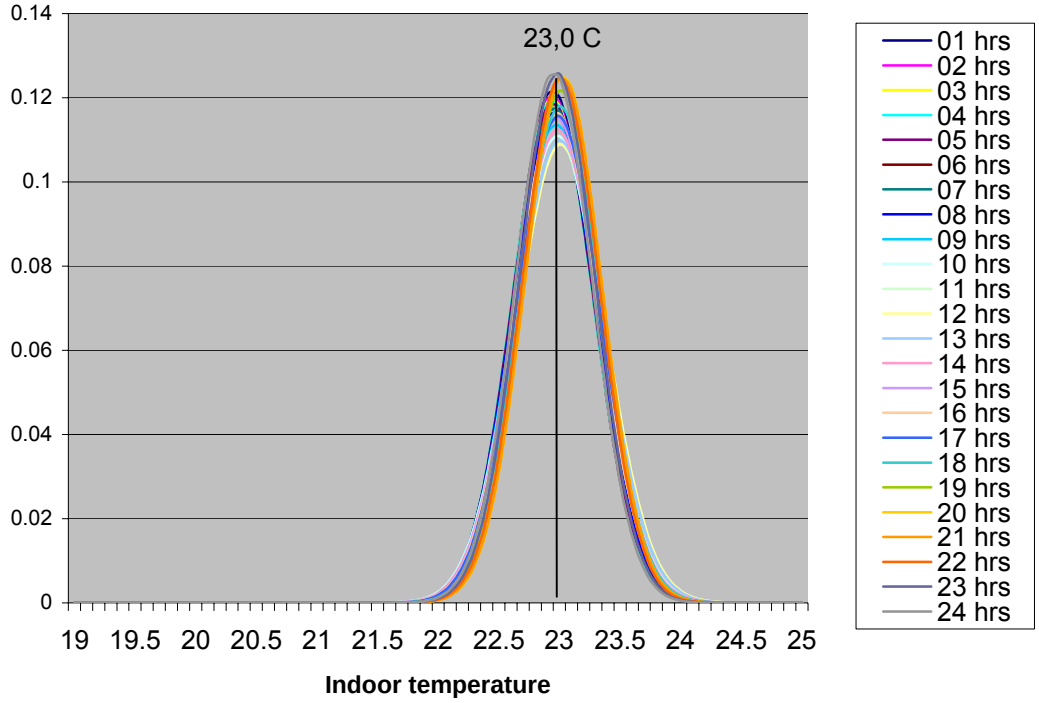

Figure A7.2 Frequency distributions of indoor temperature at each hour of the day during the heating season, February - April 2002 and September 2002 - January 2003

3 Meteorological data

The ENLOSS model uses hourly meteorological data of the following variables:

- Outdoor temperature
- Wind (velocity and direction)
- Solar irradiation (diffuse and direct) on vertical surfaces is calculated for each hour from meteorological data on cloudiness, visibility, atmospheric humidity and precipitation as explained in Taesler & Andersson, 1984.

The meteorological data are obtained from the meso-scale analyses system of SMHI (MESAN) except for outdoor temperature for which local observations at the building site are used. The analysed period is February 2002 – January 2003.

4 Method

The instantaneous energy demand is calculated initially hour by hour. To account for the thermal inertia of the building, this is then smoothed backwards in time (c.f section 6) using a weighting function and an estimated time constant τ of 18 hrs. The smoothed values are added to form daily totals. Negative hourly values (i.e. indicating cooling demands) are included in the daily totals. Monthly totals are calculated from daily totals, however not including negative daily values.

5 Results

Figure A7.3 shows measured and calculated daily values of the net heating demand for the whole year. Corresponding results for the months of February and October respectively are shown in Figures A7.4 and 5. Comparison of monthly net heating demands (Table A7.2) show a slight but systematic overestimation in modelled versus measured data, amounting to approximately 7 % on an annual basis.

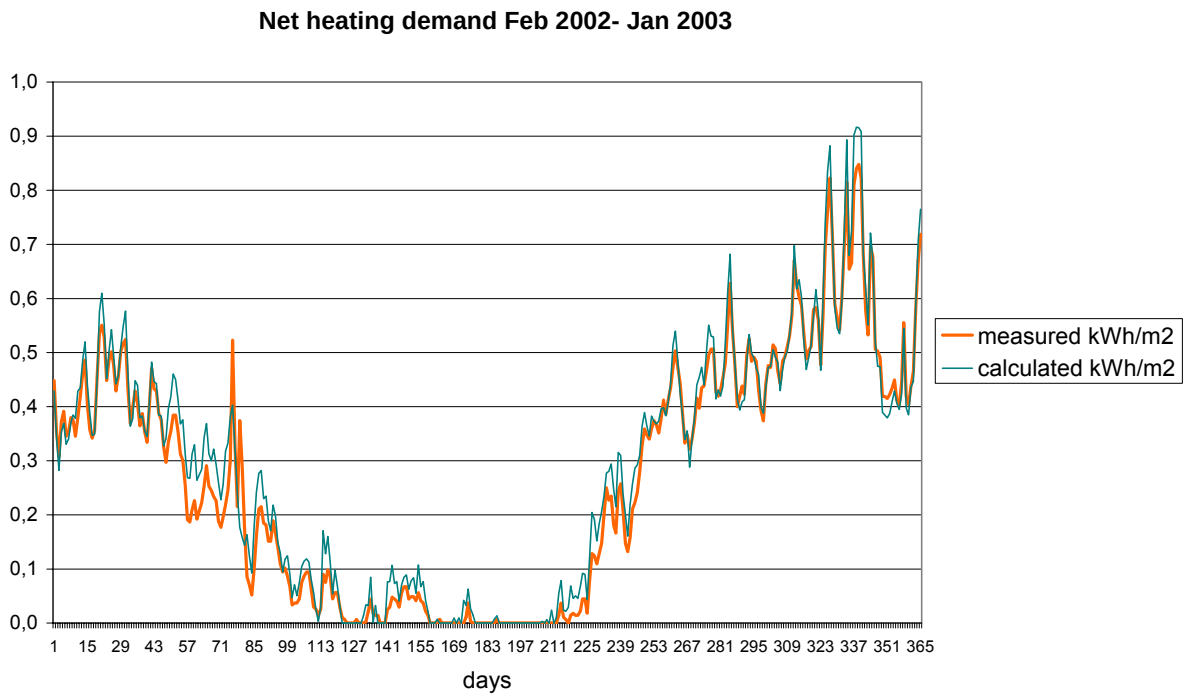

Figure A7.3 Measured and calculated net heating demand, daily values, Feb 2002 – Jan 2003.

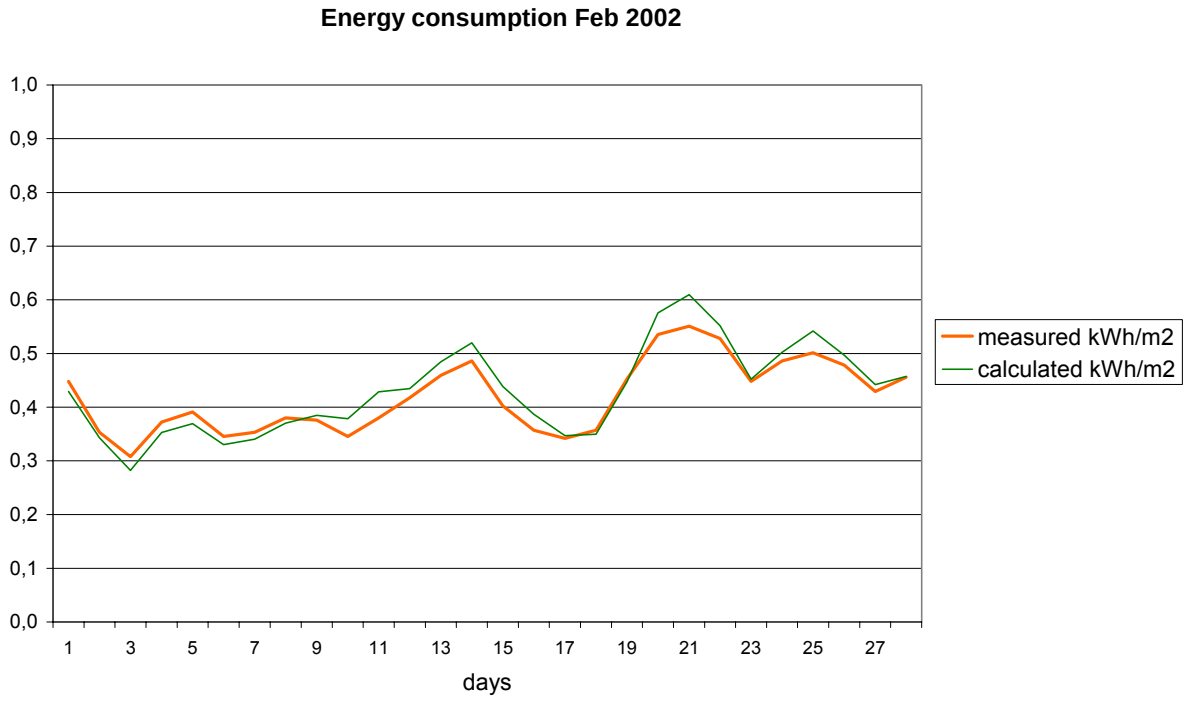

Figure A7.4 Measured and calculated energy consumption, daily values, Feb 2002.

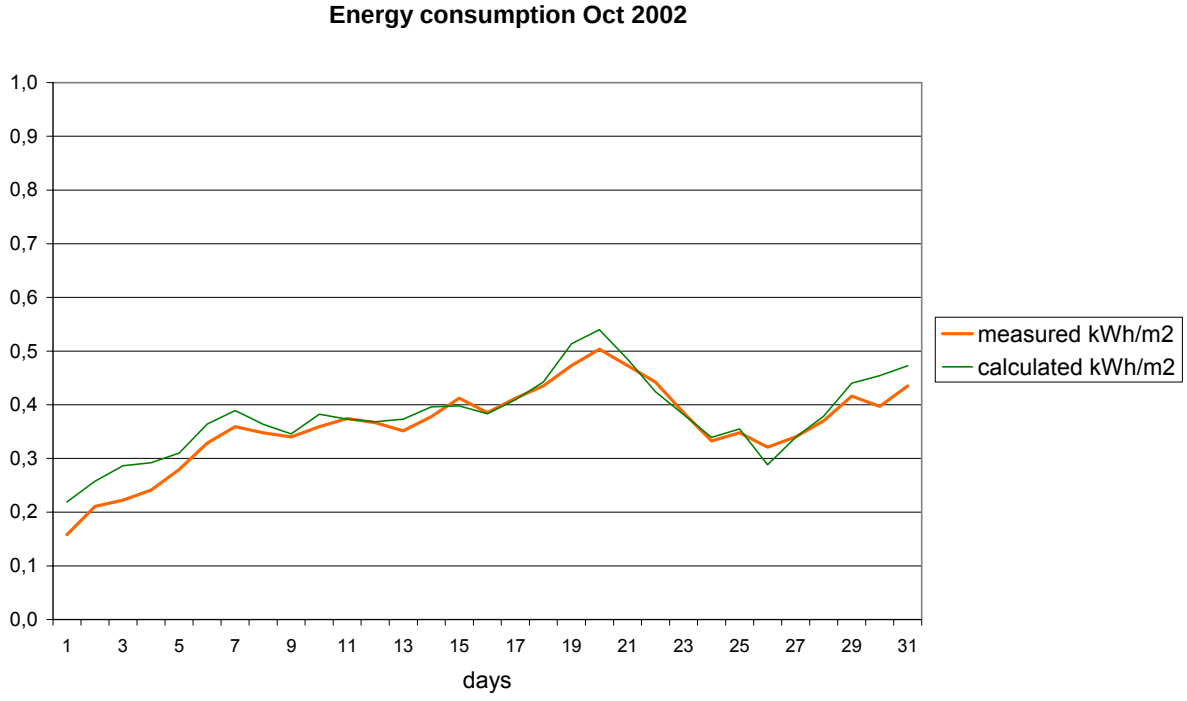

Figure A7.5. Measured and calculated energy consumption, daily values, Oct 2002.

Linear regression of calculated vs. measured net heating demand for the whole year indicates that the model explains 98 % of the variability in $q_{N,}$ cf. Figure A7.6.

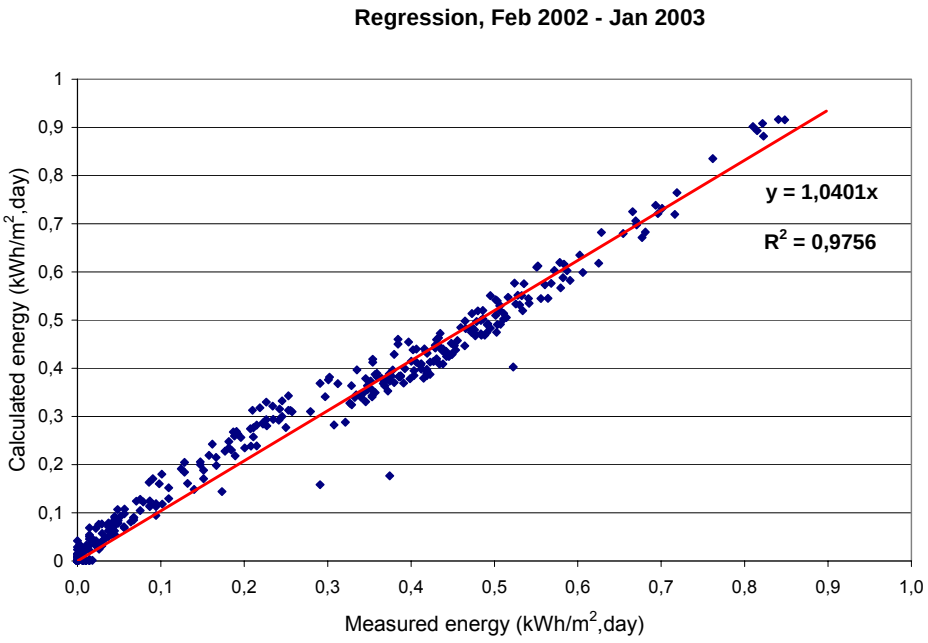

Figure A7.6 The linear regression shows the relation between calculated and measured energy.

Monthly data on net heating demand, q_N, are given in Table A7.2.

Table A7.2. Comparison between calculated and measured net heating demand, monthly values (kWh/m^2) February 2002 – January 2003.

	Calculated	Measured
Feb	12.05	11.74
Mar	12.45	11.41
Apr	7.90	6.67
May	3.40	2.61
Jun	0.99	0.62
Jul	0.74	0.37
Aug	0.06	0.01
Sept	4.54	3.22
Oct	11.77	11.20
Nov	14.33	14.08
Dec	18.41	18.11
Jan	17.64	17.37
∑ year	104.27	97.41

Appendix 8: Paper to the IBS

Research in Building Physics and Building Engineering – Fazio, Ge, Rao & Desmarais (eds)

Upgraded weather forecast control of building heating systems

A. Sasic Kalagasidis
Chalmers University of Technology, Gothenburg, Sweden

R. Taesler, C. Andersson & M. Nord
Swedish Meteorological and Hydrological Institute (SMHI), Norrköping, Sweden

ABSTRACT: As part of its customer service, the Swedish Meteorological and Hydrological Institute (SMHI) provides a short-range weather forecast for a building heating system control automatization. The aim of the service is to minimize heating surpluses by utilizing solar energy and other casual heating gains when they are available, and to make a better balance of extra heating demands during, for example, windy days. This method is based on an energy budget model of a building and opposes commonly used control methods based on prevailing outdoor air temperature. Several years of experience in Swedish buildings show typical energy savings of 10–20 kWh/m^2 year. The model also enables improved follow up and normalization of monthly and yearly energy use. Apart from processing weather data, the model calculates a building heating demand using the thermal response method. This paper shows verification results of the building thermal model and discusses its possible improvements.

1 INTRODUCTION

1.1 *Background*

The Swedish Meteorological and Hydrological Institute (SMHI, the national meteorological service of Sweden), has a long-term interest in studies of interactions of atmospheric and built environments. This includes both interdisciplinary research and development of customer-oriented services.

Increase in energy prices as well as growing concern about effects of green house gas emissions constitute strong arguments for the SMHI to contribute to a more efficient use of energy by developing applications of weather and climate information. In particular, energy performance of a building has been identified as an important area in this context.

Traditional methods in building energy management account only approximately for impacts of weather and climate. Assessments of building energy requirements in the design stage, as well as in monitoring and normalization of energy usage, are still frequently based on heating or cooling degree days or hours. Real time heating control systems usually respond only to changes in outdoor air temperature. Neglecting the effects of other prevailing meteorological conditions on the heat balance of building results in uncontrolled variations in indoor temperature and/or excessive use of energy for heating or cooling.

The approach described below takes into account the effects of weather and climate and offers improved efficiency in energy use for indoor climate control and, also, precision in building energy monitoring.

1.2 *The SMHI building energy model system*

A system of models (ENLOSS) has been developed for studying of impact of weather and climate on the building heat budget (Taesler et al., in press). The core of the system is a building energy model, which calculates hourly heat losses and gains due to the combined action of outdoor temperature, wind, solar irradiation and precipitation. It also includes building thermal characteristics and internal "free gains" from occupants and electric appliances. The meteorological input to the calculations (observations and forecasts) is adjusted to account for physical conditions on the local (urban) and micro (building site) scale.

An equivalent outdoor temperature T_e is defined by postulating a linear relation between the specific net heating power q_n (W/m^2) needed to maintain a prescribed indoor temperature T_{in} and the difference $(T_{in} - T_e)$ according to Equation 1:

$$q_n = K \cdot (T_{in} - T_e) \tag{1}$$

where K (W/m^{2}K) = building characteristic heat transfer coefficient; T_e (°C) = equivalent outdoor temperature.

By means of regression analysis on q_n vs. meteorological data, an explicit equation for T_e is obtained as a function of the outdoor temperature T_{out}, wind

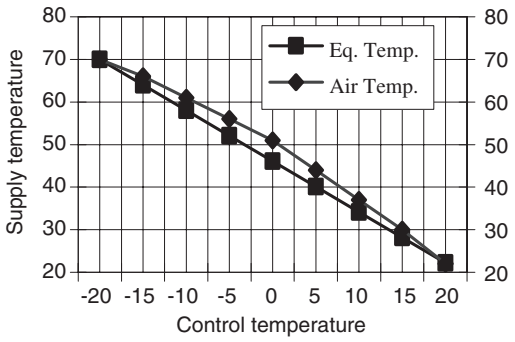

Figure 1. Building heating power control according to the equivalent and the outdoor air temperature.

v (m/s) and solar radiation S, also including the heat loss to the ground G and internal "free energies" from electric appliances E and occupants P (all in W/m^2):

$$T_e = T_{out} - \alpha \cdot (\beta \cdot v^2 \cdot \Delta T + G - S - E - P) \qquad (2)$$

Here, the regression coefficients α and β represent specific building categories.

The difference $T_{in} - T_e$ may show significant deviations (both positive and negative) from the corresponding difference between the indoor and outdoor air temperature $T_{in} - T_{out}$.

Experience shows that T_e exceeds T_{in} quite frequently, even during the main heating season. This indicates a heat surplus that may increase indoor temperatures and, eventually, also require energy for cooling. Calculations with the ENLOSS–model show that the total sum of this heat excess may amount to approximately 25% of the total heat loss of a building during the heating season.

1.3 *Applications of the equivalent temperature concept*

1.3.1 *Predictive control of building heating systems*

T_e is used to replace T_{out} as input to automatic building heating control systems. This is illustrated in Figure 1 by control curves for the heating power (i.e. the supply temperature of the heating system) according to T_e and T_{out} respectively. The curvature of the T_{out} control curve is a common feature due to the non-linear relationship between heat release by the heating system and supply temperature (see for example ASHRAE 1997b). In practice the non-linearity often results from empirical adjustments made by working staff in response to complaints from occupants. Such complaints are frequent at outdoor temperatures around 0°C, a temperature range characterized by frequent weather variations associated with cyclone activity.

The aim is to optimize the heating process by supplying the heating power required to keep the building as closely as possible in thermal balance at the prescribed temperature (usually +21°C). To achieve this, a predictive control strategy has been developed, whereby T_e is calculated from meteorological forecast data. The rationale behind this approach is as follows.

By intentional underbalancing of the building heat budget, i.e. by reducing heating power prior to situations when $T_e > T_{out}$ (e.g. before sunrise) the excess heat may be turned into useful heat instead of causing overheating. Conversely, when $T_e < T_{out}$, heat deficits are compensated, and thus, lowered indoor temperatures are avoided.

To utilize the potential of predictive control it is important to make use of building heat storage. This is done by using a thermal time constant of the building in order to filter the instantaneous series of forecasted T_e, and also by applying a forward time shift of several hours.

T_e is produced daily by the SMHI, and also for five days ahead. The forecasts are distributed to customers via the Internet. Predictive control has been offered for some years by SMHI as a service in collaboration with several private Swedish companies. Experience from a large number of cases shows annual energy savings typically in the range of 5–20%, approximately corresponding to 10–20 kWh/m^2/yr, while maintaining stable indoor temperatures close to prescribed values.

Figure 2 shows a detailed comparison of daily differences in net heating usage and in mean indoor temperatures for two identical multistory residential buildings in Köping, Sweden, respectively. The data cover four months of operation (September 2004–January 2005). Both buildings, each having a heated floor area of 2633 m^2, are served by a district heating system. One of the buildings is used for testing of the forecast control, while the other one serves as a reference. Indoor temperatures and total heat usage (i.e. both space heating and hot water production) are monitored on an hourly basis. Evaluation of forecast control performance has shown as annual net saving of energy for space heating of 8%. Indoor temperature is very close to the required value (+22°C) in both buildings. Over the period shown in Figure 2, the test building is 0.1°C warmer on the average with 9% lower energy usage.

1.3.2 *Monitoring and normalization of energy usage*

Traditionally, heating degree-days have been used to normalize statistics on energy use. As long as the heating power is controlled only by outdoor air temperature, a high degree of agreement between variations in energy use and variations in heating degree-days is to be expected. However, such agreement is not a proof for optimal energy efficiency, but does, in fact, indicate possibilities for the improved energy use. To overcome the limitations of the traditional heating-degree

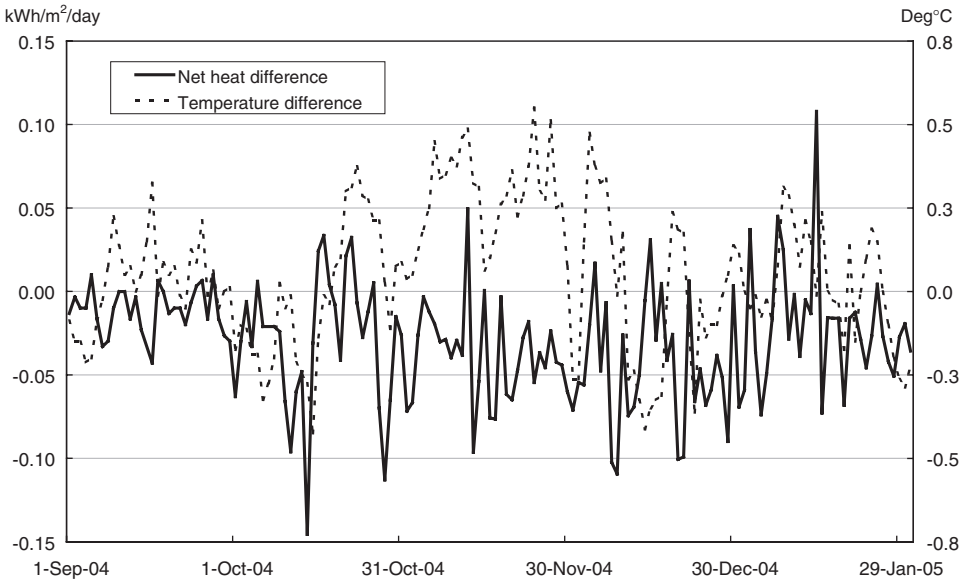

Figure 2. Comparison of differences the net energy use for space heating and indoor air temperatures in the test and the reference building (test – reference).

concept (see for example ASHRAE 1997a), daily averages of $\overline{T}_e$ are used to compute the so called "equivalent heating degree-days" D_H:

$$D_H = \sum \left(T_{in} - \overline{T}_e \right) \tag{3}$$

By dividing the present value of D_H with the corresponding long-term one $\overline{D}_H$, which covers a period of over thirty years, the so-called "Energy-Index" *EI* is obtained. This number represents a relative measure of the energy used for heating during a particular period. This is used in analogy with the corresponding relative numbers of traditional heating degree-days, aiming to normalize data on energy use.

EI shows considerably less variability than relative traditional heating degree-days. This is evident in particular during the beginning and the end of the heating season, where traditional heating degree–days frequently show totally unrealistic changes from one month or one year to another.

As with T_e- forecasts, *EI*-data distinguish different building types. Both actual and normal equivalent degree-days are computed assuming optimal performance of the heating control system, and by maintaining a balanced energy budget and a stable indoor temperature. Besides, comparisons with the actually measured changes in energy use serve to detect malfunctions of the heating system. In practice, it is common to use a standardized building or an "average" building type to represent groups of buildings, built up areas or even entire district heating systems.

2 POSSIBILITIES FOR IMPROVING THE ENLOSS – SYSTEM

2.1 *Present limitations and weaknesses*

The ENLOSS-model represents an attempt to integrate atmospheric and building sciences. Compared to other building energy models, ENLOSS is rather advanced for its meteorological input. However, evaporation and long wave radiative exchange have not so far been included explicitly in the heat budget.

The processes of energy exchange due to heat transfer, ventilation, infiltration and solar radiation between a building and its surrounding atmosphere are not simulated dynamically, but described by analytical functions. Also, certain simplifications are made in the description of building structures and thermal properties.

Calculations of the heat budget of a building by the ENLOSS-model for the heating season indicate heat excesses, corresponding to maximum possible reductions of the net heat requirement of approximately 25%. Practical applications of the ENLOSS-model for a predictive control of heating systems so far produce savings typically ½ of this value. To improve performance of predictive control and to develop the model further, the SMHI has established collaboration with the Building Physics Division of Chalmers University of Technology in Gothenburg, Sweden. This involves, among other things, verification of the ENLOSS-model against other building energy models.

2.2 *The ENLOSS thermal model of a building*

Essentially, the task of the ENLOSS model is to evaluate dynamical heat losses from a building under given circumstances. To calculate a space heating demand directly by heat balance procedures requires a laborious solution of energy balance equations for the indoor air, surrounding building envelope, infiltration and ventilation air and internal energy sources. Computer programs, where instantaneous heating demands are calculated in this exact manner, are nowadays substantially developed concerning the level of complexity and the calculation speed. Yet, they are still impractical for the everyday use on a large number of buildings. The ENLOSS processes the data daily for hundreds of buildings and for every hour in a day, using the transfer function concept as a simplification compared to the strict heat balance procedure. The transfer function or the thermal response calculation concept is a known method for space cooling load calculations (ASHRAE 1997a), because of the clearly transient nature of the problem. The same procedure is valid for the space heating calculations and details regarding the ENLOSS model are given hereafter.

Having a constant indoor air temperature, the calculation of dynamical heat losses for a building turns into determining its effective outdoor temperature. This temperature reflects not only the changes in weather parameters, but also the transient heat transfer through a building construction. It is calculated by the following equation[1]:

$$T_{eff}(t_o) = T_e(t_o) + \sum_{t=1}^{\tau} \Delta T_e(t) \cdot e^{-t/\tau} \cdot \left(1 - e^{-1/\tau}\right) \tag{4}$$

where

$$\Delta T_e(t) = T_e(t_o - t) - T_e(t_o) \tag{5}$$

Instantaneous value of T_{eff} is obtained as a weighted average of the equivalent air temperature T_e at a present and preceding time steps t_o and $(t_o - t)$, with the weighting factors that read:

$$1 - \sum_{t=1}^{\tau} e^{-t/\tau} \cdot \left(1 - e^{-1/\tau}\right) \tag{6}$$

for T_e (t_o) and

$$e^{-t/\tau} \cdot \left(1 - e^{-1/\tau}\right) \tag{7}$$

for $T_e(t_o - t)$. T_e is defined by Equation 2 and time steps t are in hours.

[1] In this work the term "effective" is used to stress that the effective temperature is the weighted equivalent temperature from Equation 2.

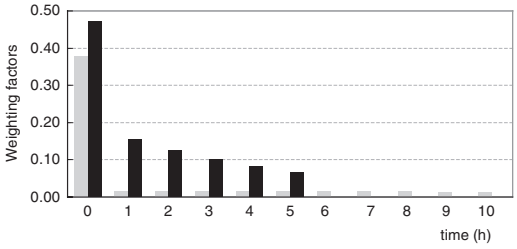

Figure 3. Weighting factors according to the ENLOSS method (Eq. 6–7) for the lightweight (black bars) and the heavyweight construction (gray bars). The number of backward steps equals the time constant of the house, e.g. 5 and 64 respectively.

τ (h) is a building time constant (see CEN 2004), which is defined under the assumption that the indoor air and internal wall layers (up to the insulation) have the same temperature.

Since the weighting procedure "moves" along the temperature array as the time progresses, it is also known as a method of moving weighted averages.

Equation 4 is particularly suitable for practical use, since it can be readily calculated by most of available programs. The heat loss from a building reads:

$$Q^E_{loss}(t_o) = \left[T_{in} - T^E_{eff}(t_o)\right] \cdot K_e \cdot A \tag{8}$$

where T_{in} = required (constant) indoor air temperature; K_e (W/m^{2}K) = overall heat conductance of a building; A (m^2) = total (internal) area of the building. The letter "E" in the superscript denotes that the quantity is calculated by the method presented (to be called here the "ENLOSS" method).

To illustrate the weighting method, the hourly-averaged weighting factors for the two model houses are given in Figure 3. The houses are extremely trivial – boxes "hanging" in the air with only one type of the wall. They have the same overall heat transfer coefficient of 0.51 W/m^{2}K, but they differ in the wall mass: the lightweight wall consists of wood siding (0.009 m) underlined by insulation (0.066 m) and gypsum board (0.012 m) and the heavyweight is made of wood siding (0.009 m), insulation (0.062 m) and concrete (0.1 m).

2.3 *Verification of the ENLOSS thermal model*

The verification procedure involves running calculation exercises, which are based on standard tests for building energy simulation programs (such as BESTEST, (IEA 1995)). Calculations performed by the ENLOSS method are compared to two different solutions. The first solution comes from a numerical program (Sasic 2004), where the heating energy demand of a building is calculated directly from a system of energy balance equations for all involved components. The transient heat transfer through walls is

calculated as one-dimensional process and the indoor air is treated as well mixed. The numerical solution is based on the control volume technique. The program is verified (Sasic, in prep) and the solution obtained (denoted here with "NM" – numerical model), will be the reference solution in this analysis.

The second solution comes from a theory of Dynamic Thermal Networks (DTN) (Claesson 2002, Wentzel 2003). It deserves a special attention here, since it also involves the method of moving weighted averages for calculation of the effective outdoor temperature. However, the weighting factors κ (-) are calculated from a basic step-response solution:

$$\kappa(t) = \frac{1}{K} \cdot \frac{dq(t)}{dT} \tag{9}$$

where q (W/m^2) = heat loss from a wall when the outdoor temperature suddenly drops from one to zero while the indoor temperature remains one; K (W/m^{2}K) = heat conductance of a wall.

Note that the heat flux $q(t)$ is actually a response function of a system (a wall or a whole building). The function should be calculated only once, either analytically (see for example Carslaw & Jaeger 1959) or, as it is the case here, by the numerical program involved (Sasic 2004).

The effective outdoor temperature for a building component i reads:

$$T_{eff,i}(t_o) = \int_{-\infty}^{t_o} \kappa_i(t_o - t) \cdot T_{out}(t) dt \tag{10}$$

and the heat loss from a whole building is:

$$Q_{loss}^{DTN}(t_o) = \sum_i K_i \cdot A_i \cdot \left[T_{in} - T_{eff,i}^{DTN}(t_o) \right] \tag{11}$$

where K_i and A_i = heat conductance and area of a building envelope component. The "*DTN*" in the superscript denotes that the quantity is calculated by the theory of Dynamical Thermal Networks. The discrete form of the convolving integral from Equation 10 is also readily calculated in practice:

$$\begin{aligned} T_{eff,i}(t_o) &= \sum_{m=1}^{M} \kappa_i(t_o - m \cdot \Delta t) \cdot T_{out}(m \cdot \Delta t) \cdot \Delta t \\ &= \sum_{m=1}^{M} \kappa_i(m \cdot \Delta t) \cdot T_{out}(t_o - m \cdot \Delta t) \cdot \Delta t \end{aligned} \tag{12}$$

where Δt = discrete time step; m (-) = number of backward steps. The total number of backward steps M (-) is determined in order to fulfill the condition:

$$\sum_{m=1}^{M} \kappa_i(m \cdot \Delta t) = 1 \tag{13}$$

The hourly-averaged weighting factors from the DTN model are given in Figure 4, for the same model houses as in Figure 3.

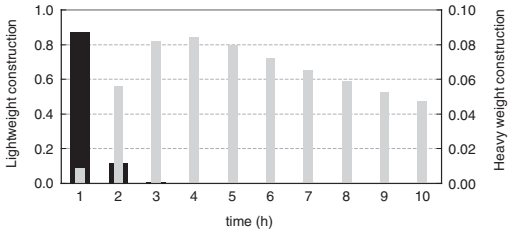

Figure 4. Weighting factors according to the DTN method (Eq. 12) for the lightweight (black bars) and the heavyweight construction (gray bars). The number of backward steps are 3 and 65 respectively.

Table 1. Annual energy consumption of the "hanging-box" house in kWh/m^2 of the floor area.

Method	Lightweight $\tau = 5$ h	Heavyweight $\tau = 64$ h
E	224	224
DTN	224	224
NM	223	223

2.3.1 *Energy balance for the "hanging-box" house*

The first calculation exercise relates to the annual heat consumption of the "hanging-box" house, i.e. the house completely surrounded by outdoor air and with one type of the wall (as already mentioned in section 2.2). These are the operating conditions: the outdoor temperature is for Gothenburg, Sweden, the indoor temperature is 21°C constantly, and no ventilation and solar radiation are introduced.

By comparing the weighting factors in Figures 3 and 4, one may expect a big disagreement in results. However, both methods give results close to the reference solution, as shown in Table 1. Even the instantaneous values of the heating demand are in a very good agreement (Fig. 5), suggesting that the solution is almost independent of the weighting method.

2.3.2 *Energy balance for the standard test house without ventilation and solar heat gains*

The second calculation exercise deals with a more realistic house with distinguished walls, floor, ceiling and two large windows on the southern side. The house is still simple in shape (the box type), but placed on the ground and oriented in space. Again, there are two model houses that differ only in the wall and floor construction (lightweight/heavyweight). Geometrical and other construction details, as well as thermal properties of the building materials are the same as in the standard calculation exercises 600 and 900, from the BESTEST test (IEA 1995). Operating conditions are the same as in the first exercise (e.g. no solar radiation or ventilation), except that the ground temperature is 10°C constantly.

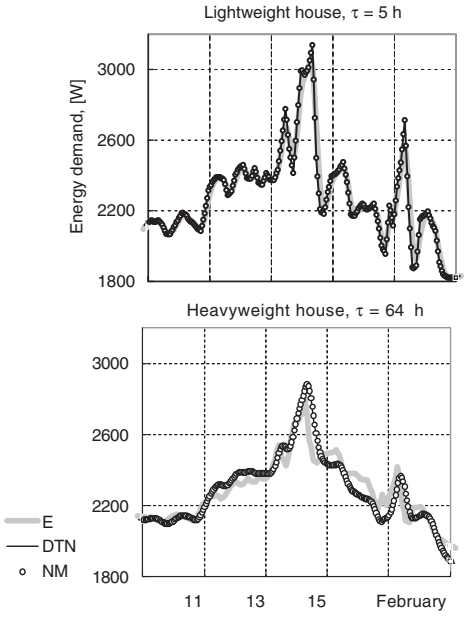

Figure 5. Instantaneous values of the heating energy demand for the "hanging-box" house, calculated by the three different methods.

Table 2. Annual energy consumption of the standard-test houses in kWh/m^2 of the floor area.

Method	Lightweight $\tau = 6$ h	Heavyweight $\tau = 29$ h
E	187	186
DTN	187	187
NM	187	187

Results, which are in excellent agreement, are shown in Table 2 and Figure 6. The weighting factors in the DTN method are calculated for each construction element separately and Figure 4 shows that the difference is not only in the size of weights, but also in the position of the dominant ones. In the ENLOSS method, all construction elements are weighted by a single thermal parameter – a building time constant, and then, always the present and the very first backward records appear as the governing temperatures. However, it seems that the solution is not influenced by the weighting method.

2.3.3 *Energy balance for the standard test house with ventilation and solar heat gains*

The test houses are the same as in Section 2.3.2 except for the fact that mechanical ventilation by the outdoor air and solar heat gains thorough the windows are introduced. In the numerical and DTN model, solar gains

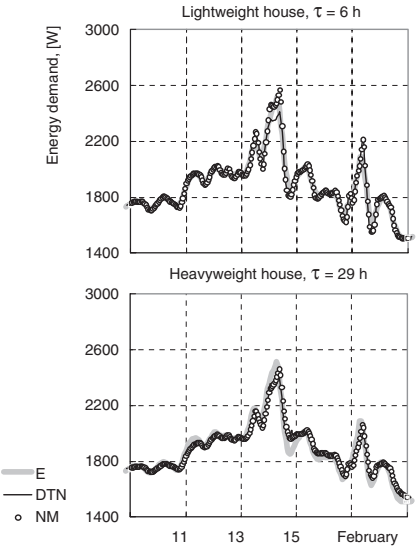

Figure 6. Instantaneous values of the heating energy demand for the standard-test house, calculated by the three different methods. No ventilation or solar radiation is introduced.

are treated as being only convective. In the ENLOSS model, both the ventilation heat losses and the solar gains are enclosed in the equivalent outdoor air temperature from Equation 2, which is calculated from Equation 1:

$$T_e(t) = T_{out}(t) + \frac{1}{K_e \cdot A}\left[g \cdot A_{window} \cdot I_{sol}(t) - G\right] \qquad (14)$$

where g = solar transmittance through glazing; I_{sol} (W/m^2) = intensity of solar irradiance; A_{window} (m^2) = glazing area; G (W) = ground heat loss. The ventilation airflow rate is kept constant and equals 0.5 h^{-1}.

The equivalent air temperature from Equation 14 is weighted by the factors from Equations 4 and 5 and, finally, the heat loss from a building is calculated by Equation 8. The overall heat transfer coefficient from Equation 14 reads:

$$K_e = \frac{1}{A} \cdot \left[\sum_i K_i A_i + \frac{n \cdot (c_p \rho)_{air} \cdot V}{3600}\right] \qquad (15)$$

where n (h^{-1}) = number of air changes per hour; $(c_p\rho)_{air}$ (J/m^{3}K) = volumetric heat capacity of air; V (m^3) = volume of the air space.

Results from Table 3 show that the annual energy consumption calculated by the ENLOSS method differs about −6% (−20%) from the other two results, for the lightweight and heavyweight house respectively.

Table 3. Annual energy consumption of the standard-test houses with ventilation and solar radiation, in kWh/m^2 of the floor area.

Method	Lightweight $\tau = 5$ h	Heavyweight $\tau = 25$ h
E	175	146
DTN	186	183
NM	186	182

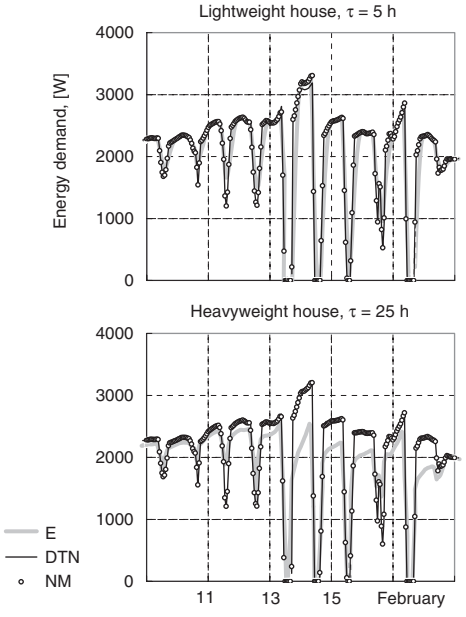

Figure 7. Instantaneous values of the heating energy demand for the standard-test house with ventilation and solar radiation, calculated by the three different methods.

The instantaneous values in Figure 7 explain that ENLOSS gives results with the same profile and dynamics as the other two methods, but it seems that the effect of thermal inertia of the building is overestimated and especially for the heavy weight house.

It was shown in the two previous exercises that the weighting method does not affect the calculation of the transient heat transfer through walls. In the ENLOSS solution solar heat gains appear as the only new value to be weighted (see Eq. 14). Accordingly, they are not direct (or convective) gains to the air as it is the case in the NM and DTN solutions. Therefore, additional test is performed – the same calculation exercise is considered, but the solar gains are treated as radiative heat sources also in the control methods. It is assumed that these gains are uniformly distributed between internal surfaces (since the same is valid for the ENLOSS method). Heat transfer between internal surfaces and the air is described with one (combined) surface film transfer coefficient.

Table 4. Annual energy consumption of the standard-test houses with ventilation and solar radiation, in kWh/m^2 of the floor area. Solar gains are treated as radiative heat sources.

Method	Lightweight $\tau = 5$ h	Heavyweight $\tau = 25$ h
E	185	159
DTN	187	162
NM	186	165

For the DTN method, the transfer function for the solar gains as radiative heat sources is found in a similar way as the one for the outdoor air temperature (see Eq. 12):

$$I_{sol,rad,i}(t_o) = \sum_{m=1}^{M} \kappa_{sol,i}(t_o - m \cdot \Delta t) \cdot I_{sol}(m \cdot \Delta t) \cdot \Delta t \tag{16}$$

where $I_{sol,rad,i}$ = net solar energy transferred to the air from a building component i; κ_{sol} = solar weighting factors calculated by Equations 9 and 13. Details may be found in Sasic et al. (2005).

Results for this final test are summarized in Table 4. The effect of heat storage in heavyweight walls is seen as a substantially smaller heating demand for the heavyweight house (compared to the ones in Table 3). Consequently, the difference between the ENLOSS method from Table 3 and the DTN and NM methods from Table 4 is −8% for the heavyweight house. Note that results for the lightweight house remain unchanged.

The same weighting method for the solar gains (Eq. 16) is applied in the ENLOSS model and new results are shown in Table 4. As it can be seen, an excellent agreement is obtained between all three methods, which is also confirmed by the comparison of instantaneous values in Figure 8. Thus, the difference in treating solar gains by the models explains the difference in the results from Table 3. A definition of the equivalent temperature from Equation 14 and the weighting method that follows are quite common procedures in simplified models, to assess, for example, a free-floating indoor temperature (Burmeister & Keller 1998). It is shown here that the procedure may be improved by using more detailed transfer functions.

3 CONCLUSIONS

At present, the ENLOSS-model performs well in practical applications, achieving significant savings in annual heat requirement as well as in maintaining a stable indoor temperature. Theoretical considerations

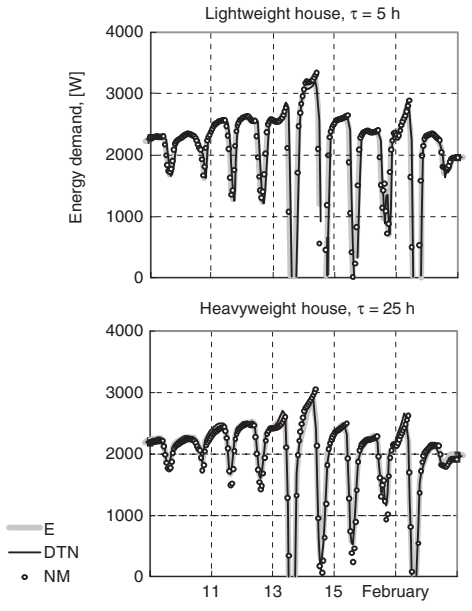

Figure 8. Instantaneous values of the heating energy demand for the standard-test house with ventilation and radiative solar gains, calculated by the three different methods.

and numerical validations, however, suggest a potential for further improvements in the performance of the model.

The equivalent and the effective outdoor temperature are crucial outcomes of the ENLOSS model. The first is already advanced for its meteorological input of real data and the precision is further enhanced by inclusion of local (urban) and micro scale (building) climate effects that significantly influence the results. The second, i.e. the effective outdoor temperature, represents the weighted average of the equivalent one, in order to account for dynamical effects of the heat storage in a building envelope.

The weighting factors used in ENLOSS are shown to be approximate in comparison with the exact ones calculated by the theory of Dynamical Thermal Networks. For problems where only the transmittive heat losses through a building envelope are concerned, the ENLOSS model gives results that are in excellent agreement with the two control solutions: the one coming from a numerical model and the other from the theory of Dynamical Thermal Networks. For problems where transmitted solar radiation through windows is involved, a good agreement is achieved. Furthermore, it is shown that these gains should be treated as the radiative ones in the control methods and that the accuracy of the ENLOSS procedure for solar gains may be improved by using more detailed transfer functions.

The work presented is an excerpt from an ongoing verification study of the ENLOSS model (Sasic et al. 2005). In future, the study will address other parameters such as heat losses due to infiltration, longwave radiation heat exchange with surroundings and evaporation of moisture from surfaces.

REFERENCES

ASHRAE. 1997a. *Handbook of fundamentals*. American Society of Heating, Refrigerating and Air Conditioning Engineers, Atlanta, USA.

ASHRAE. 1997b. *HVAC Systems and Equipment*. American Society of Heating, Refrigerating and Air Conditioning Engineers, Atlanta, USA.

Burmeister, H. & Keller, B. 1998. Climate surfaces: a quantitative building-specific representations of climates. *Energy and Buildings* (28): 167–177.

Carslaw, H.S. & Jaeger, J.C. 1959. *Conduction of Heat in Solids*. 2nd ed. Oxford: Oxford University Press.

CEN. 2004. EN ISO 13790. Thermal performance of buildings – Calculation of energy use for space heating. European Committee for standardization. Brussels, Belgium.

Claesson, J. 2002. Dynamic Thermal Networks. Outlines of a General Theory. Building Physics in the Nordic Countries. Proceedings of the 6th Symposium. Trondheim, Norway.

IEA International Energy Agency 1995. *Building Energy Simulation Test* (BESTEST) *and Diagnostic Method*. National Renewable Energy Laboratory, Golden, Colorado.

Taesler, R., Andersson, C. & Nord, M. (in press). Optimizing energy efficiency and indoor climate by forecast control of heating systems and energy management in buildings. Report RMK 107. Norrköping: SMHI.

Sasic Kalagasidis, A. 2004. *HAM-Tools. An integrated simulation tool for Heat, Air and Moisture transfer analyses in Building Physics.* Doctoral thesis. Chalmers University of Technology, Gothenburg, Sweden. ISBN 91-7291-439-4. Computer program is available for free downloading on www.ibpt.org.

Sasic Kalagasidis, A., Nord, M. & Andersson, C. 2005. SMHI common exercise 0. Calculation of energy use for space heating. Chalmers University of Technology, Gothenburg, Sweden. Report 2005:6. ISSN 1652-9162

Sasic Kalagasidis, A. (in prep). HAM-Tools testing with ANSI/ASHRAE Standard 140-2001 (BESTEST).

Wentzel, E-L. 2003. Application of the theory of dynamic thermal networks for energy balance of a building with three-dimensional heat conduction. *Research in Building Physics*. The Netherlands: Balkema.

BIBLIOGRAPHY

Norford, L.K. & Reddy, A.T. 2004. Proposed Tools and Capabilities for Proactive Multi-Building Load Management: Part 2 – Aggregated Operation. ASHRAE Transactions 101 (2).